Energy Conversion and Management: X 16 (2022) 100322

Contents lists available at ScienceDirect

Energy Conversion and Management: X

journal homepage: www.sciencedirect.com/journal/energy-conversion-and-management-x

Oscillating-water-column wave energy converters: A critical review of numerical modelling and control

M. Rosati [a,*], J.C.C. Henriques [b], J.V. Ringwood [a]

[a] Centre for Ocean Energy Research (COER), Maynooth University, Co. Kildare, Ireland
[b] IDMEC, Instituto Superior Técnico, Department of Mechanical Eng., Universidade de Lisboa, Av. Rovisco Pais, 1049-001 Lisboa, Portugal

ARTICLE INFO

Keywords:
Wave energy
Oscillating water column
Control
Power take-off
Air turbines

ABSTRACT

Wave energy is a significant untapped renewable energy source which can be harnessed by wave energy converters (WECs). The oscillating water column (OWC) is one of the most promising WECs, due to its relative simplicity of operation and relatively small number of moving parts, all located above the water level. OWC power take-off systems also have lower levels of mechanical stress and more easily dissipate excess wave power, compared to other types of WECs, helping to increase the capacity factor. To improve the economic viability of OWC WECs, the performance of the associated energy-maximising control system is a major determining factor. However, energy maximisation alone does not necessarily imply that the *economic return* is maximised, since: (i) capital and operational costs of the OWC system should be considered and (ii) the additional goals of power quality and device integrity are also important. Indeed, to maximise return on investment, the optimisation pathway should ideally minimise the levelised cost of energy (LCoE). This critical review aims to: (i) provide a comprehensive analysis of the OWC control problem, (ii) offer an exhaustive review of available control strategies for OWCs, (iii) identify unexplored control and optimisation possibilities, and (iv) suggest future directions for OWC control. Ultimately, this review highlights that, to date, OWC control mainly focuses on turbine control, especially due to the importance of operating the turbine around its maximum efficiency point. However, *comprehensive* control strategies should maximise the overall, or wave-to-wire (W2W), efficiency of the device. To this end, *control-oriented* (complete and computationally simple) W2W OWC models should be considered in model-based control strategies. Finally, control co-design techniques should be adopted to guarantee optimal *control-informed* WEC design and to take into account cost-related aspects.

1. Introduction

A vast number of wave energy converters (WEC) types have been contrived to harness wave power, and one of the most promising is the oscillating water column (OWC). The OWC conception is typically attributed to Yoshio Masuda (1925–2009) [1], although an early OWC patent was filed in 1799 by Girard [2].

The essential OWC principle of operation is common to all OWC devices. The typical shape of an OWC device resembles an open-bottomed hollow structure, in which an air volume is confined inside a pneumatic chamber, Fig. 1. The displacement of a contained water column, excited by incident waves, alternatively compresses and decompresses the air volume. Since the pneumatic chamber is connected to the atmosphere, a bidirectional air flow is generated and used to drive an air turbine. The OWC power-take-off (PTO) system consists of an air turbine connected through a shaft to an electrical generator controlled by a back-to-back (B2B) converter, ultimately transferring the WEC kinetic energy into electricity to the power grid or battery banks [3]. Recently, small scale OWCs have also been employed to provide on-board power for sensors and data transmission, in remote sensing applications [3].

OWC devices fall into two main categories: fixed and floating. Fixed OWCs are usually single structures, Fig. 1 a). To reduce cost, another possibility is to incorporate multiple OWCs into breakwaters, as with the Mutriku wave power plant [4]. Other fixed OWC configurations include U-OWCs [5] and vented-OWCs (half-cycle energy extraction through a unidirectional turbine with a stop valve) [6]. A larger diversity of technical solutions exits for floating OWCs. Particularly the spar-buoy [7] and the Backward Bent Duct Buoy (BBDB) [8], Fig. 1 b) and c), have reached the prototype stage. A comprehensive review of OWC WEC types can be found in [9].

* Corresponding author.
E-mail addresses: marco.rosati.2021@mumail.ie (M. Rosati), joaochenriques@tecnico.ulisboa.pt (J.C.C. Henriques), john.ringwood@mu.ie (J.V. Ringwood).

https://doi.org/10.1016/j.ecmx.2022.100322

Available online 9 November 2022

Nomenclature

Romans

a	generator control law constant [–]
$A(\omega)$	added mass [kg]
A_v	bypass valve area [m^2]
A_∞	limiting value at infinite frequency of the added mass[kg]
b	generator control law exponent [–]
$B(\omega)$	radiation damping [N s/m]
c_{in}	speed of sound at turbine inlet conditions [m/s]
C_h	hydrostatic stiffness [kg/s^2]
C_d	discharge coefficient
d	turbine rotor diameter [m]
F_d	excitation force [N]
g	acceleration of gravity [m/s^2]
G	radiation conductance [$m^3/(Pa\,s)$]
H	radiation susceptance [$m^3/(Pa\,s)$]
h_r	radiation flow rate kernel [$m^3/(Pa\,s^2)$]
I	turbine/generator set moment of inertia[$kg\,m^2$]
k_i	impulse turbine dimensionless coefficient [–]
k_W	Wells turbine dimensionless coefficient [–]
K	radiation damping force kernel [N/m]
m_c	instantaneous air mass in the chamber [kg]
m_p	piston mass [kg]
p_{at}	absolute atmospheric pressure [Pa]
p_c	absolute air chamber pressure [Pa]
P_{elec}	electrical power [W]
P_{ctrl}^{lim}	generator electromagnetic power [W]
P_{gen}^{rated}	generator rated power [W]
P_{pneu}	pneumatic power [W]
P_{turb}	turbine aerodynamic power [W]
q_{bypass}	bypass valve volumetric flow rate [m^3/s]
q_e	excitation flow rate [m^3/s]
q_r	radiation flow rate [m^3/s]
Q_{turb}	turbine volumetric flow rate at inlet conditions [m^3/s]
R	radiation damping force [N]
S	OWC waterplane area [m^2]
t	time [s]
T_{ctrl}	generator electromagnetic control torque [N m]
T_{gen}^{max}	maximum generator torque [N m]
T_{turb}	turbine torque [N m]
u_{bypass}	bypass valve control variable [–]
u_{hssv}	HSSV valve control variable [–]
u_{pitch}	blade pitch control variable [–]
$u_{throttle}$	throttle valve control variable [–]
$\mathbf{U}$	transport velocity [m/s]
v	velocity of the water column [m/s]
v_{air}	absolute air velocity upstream the turbine [m/s]
v_{tip}	blade tip speed velocity [m/s]
$\mathbf{V}$	absolute velocity [m/s]
V_0	volume of air inside the chamber in calm water [m^3]
V_c	instantaneous air chamber volume [m^3]
w_{bypass}	bypass valve mass flow rate [kg/s]
w_{turb}	turbine mass flow rate [kg/s]
$\mathbf{W}$	relative velocity [m/s]
z	OWC surface vertical position [m]
Z	WEC impedance [N s/m]
Z_{PTO}	PTO impedance [N s/m]

Greek symbols

β	relative flow velocity angle [rad]
γ	specific heat ratio of air, c_p/c_v [–]
Δt	time interval [s]
η_{turb}	turbine efficiency [–]
κ_{turb}	turbine damping [Pa s/kg]
Π	turbine dimensionless power [–]
ρ_c	air density in the chamber [kg/m^3]
ρ_{at}	air density in atmospheric conditions [kg/m^3]
ρ_{in}	air density at turbine inlet [kg/m^3]
ρ_w	water density [kg/m^3]
σ	sliding variable [rad/s]
Φ	turbine dimensionless flow rate [–]
Ψ	turbine dimensionless pressure head [–]
ω	wave frequency [rad/s]
Ω	turbine/generator set rotational speed [rad/s]

Superscripts

lim	limited value
max	maximum value
rated	rated quantity

Subscripts

at	atmospheric quantity
bep	best efficiency point
c	chamber
ctrl	control
elec	electrical quantity
gen	generator quantity
in	turbine inlet conditions
pneu	pneumatic value
ref	reference value
tip	blade tip
turb	turbine quantity

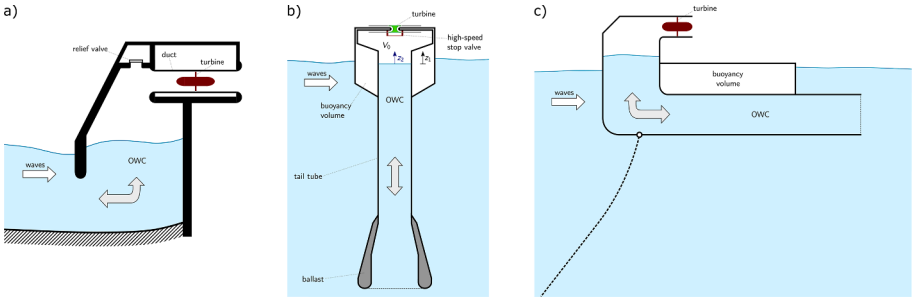

Fig. 1. Schematic representation of the three main types of OWCs: a) Fixed OWC equipped with a Wells turbine, b) Spar-buoy with a biradial turbine installed, and c) Backward Bent Duct Buoy (BBDB) with a Wells turbine fitted.

OWCs are traditionally equipped with self-rectifying air turbines that convert pneumatic to mechanical energy with bidirectional air flow. Conventional turbines can be used, providing the air flow is rectified through a set of valves. This solution is not a popular alternative to self-rectifying air turbines due to the significant aerodynamic losses associated with valves and the additional complexity of the system [10]. The installation of water turbines in OWCs is not a viable solution due to the low rotational speeds (about 150 times lower than air turbines) and the possible occurrence of cavitation, see A. A review and comparison of air turbines for wave energy applications can be found in [10,11]. Fig. 2.

To sustain the development of OWCs, it is imperative to improve the economic viability of these devices and, to this end, the design of effective control strategies is critical to achieve this purpose. The ultimate goal of the control is neither maximisation of produced power, or system efficiency, but rather to guarantee maximum economic profits. The control strategy should ideally minimise the levelised cost of energy (LCoE) defined as

$$\mathrm{LCoE} = \frac{\mathrm{CapEx} + \mathrm{OpEx}}{\mathrm{Producedenergyoverlifetime}}, \tag{1}$$

representing the final energy cost to the buyer, to enhance return on investment [12]. In opposition to the case of energy from fossil fuels, we note that wave energy is free, but the cost of converting it into a useful form is not. Different authors have examined the factors which affect the LCoE and possible pathways to reduce cost in wave energy conversion [13,14]. Minimisation of the LCoE is an unstructured and device-specific optimisation problem. A broader control co-design approach may help to incorporate some critical aspects, such as impact of the control action on operational costs (OpEx) [15], into the control strategy, while the parasitic energy cost of control actions can also be considered [16]. Generally, there is a reasonably direct relationship between CapEx and device design parameters [17]. In wave energy projects, examples of co-design problems are the selection of a suitable electric generator [18], the optimisation of the mooring line in floating power plants [19], and the selection of the type of control valves [20].

Since LCoE minimisation is, as a performance objective, very complicated, especially due to estimation difficulty of operational costs. Most wave energy studies focus on a simpler control objective, namely maximising energy production. To this end, control strategies should focus on maximising the performance of the entire OWC energy conversion chain, Fig. 3, considering the complete wave-to-wire (W2W) system model [21].

Another issue concerns the time required to complete the control action. In OWC devices, the control actions are the control of the generator electromagnetic torque, the actuation of control valves (if installed), and the pitching angle of the rotor/stator turbine blades (for certain turbine types). The actuation of blade pitching mechanisms and control valves cannot be assumed instantaneous and, consequently, their finite response time may negatively impact, or completely invalidate, the effect of the control strategy. In some cases, the control action can be anticipated (through prediction) to offset control actuation delays [22].

Although this review mainly focuses on device-side control, it should be noted that B2B power converters, which connect the generator to the power grid, provide a natural way to decouple grid-side control and device-side control at the DC-link level [23]. As such, the device-side control problem, i.e., produced power maximisation, can be considered in isolation.

Since OWC turbine efficiency characteristics generally have a pronounced maximum, the majority of reported OWC control strategies typically aim to maximise turbine efficiency (rather than converted electrical energy) while keeping the device, and its components, within a safe operational range. To this end, the turbine characteristic (a function of instantaneous chamber pressure) is interrogated to determine the optimum turbine rotational speed, which is then followed by a velocity following control loop. However, this popular control strategy, although focusing on a key system characteristic, neglects the characteristics of the generator and the hydrodynamic performance of the OWC, which may not share an optimal operating condition with the turbine. In particular, hydrodynamic damping is a strong feature in many WEC control studies [24], though is more difficult to control in OWCs. The objectives of the control action can be split into two distinct, yet interconnected, parts: a primary objective, or performance optimisation (which is the focus of this review), and complementary objectives, related to power quality and safety-related constraints (often termed *supervisory control*).

Although one can find reviews [25], comparative studies [26,27] and books [24] on control strategies for generic wave energy applications, there is a relative lack of specific material on OWC control. This work aims to provide a comprehensive analysis of the control problem for OWC devices, a review of control strategies for OWCs, suggesting future directions for OWC control.

The remainder of the paper is organised as follows. In Section 2, advantages and disadvantages of OWCs are discussed. Section 3 provides an insight into possible modelling approaches for OWCs, relating to model-based control design. Section 4 presents the PTO components and how their operation affects control. The main review analysis on OWC control strategies is presented in Section 5, with a summary in Section 6. Section 7 is dedicated to possible future directions in OWC control, while conclusions are drawn in Section 8.

2. Advantages and disadvantages of OWCs

OWC devices present several advantages over other WECs, particularly the minimal number of moving parts in a typical OWC PTO system: an air turbine and a standard generator, in the simplest configurations. Furthermore, these components are located above the water surface, therefore improving device reliability and simplifying maintenance.

The OWC is probably the WEC with the highest PTO rotational speeds, implying the lowest torques and stresses compared to other devices with the same power. The relatively high rotational speed also allows the generator to operate at high efficiency, removing the need for a gearbox. In terms of indicative numbers, the order of magnitude of the OWC free surface velocity is about $\mathscr{O}[v] \sim 10^0\,\mathrm{m/s}$. Due to the ratio of areas between the turbine duct and OWC free surface area, the absolute air velocity upstream of the turbine rotor, v_{air}, is about $\mathscr{O}[v_{\mathrm{air}}] \sim 10\,\mathrm{m/s}$. As such, the typical order of magnitude of the turbine rotational speed is about $\mathscr{O}[\Omega] \sim 10^2$,rad/s, allowing an off-the-shelf electrical generator to be connected to the turbine shaft, without a gearbox.

In addition to lower stresses on the PTO system, the spring-like effect

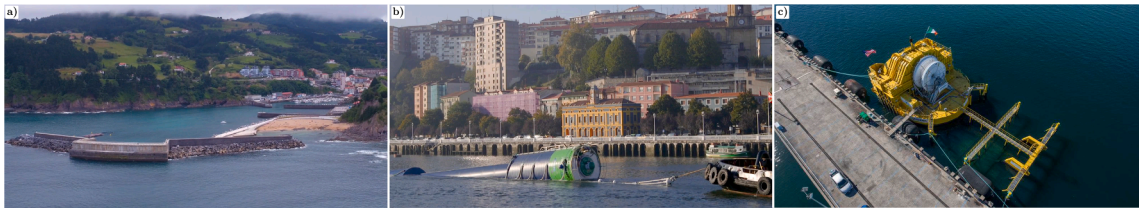

Fig. 2. Examples of the three main types of OWCs: a) Mutriku wave power plant, Basque Country, b) IDOM Marmok-A5 spar-buoy, and c) OceanEnergy OE35 BBDB.

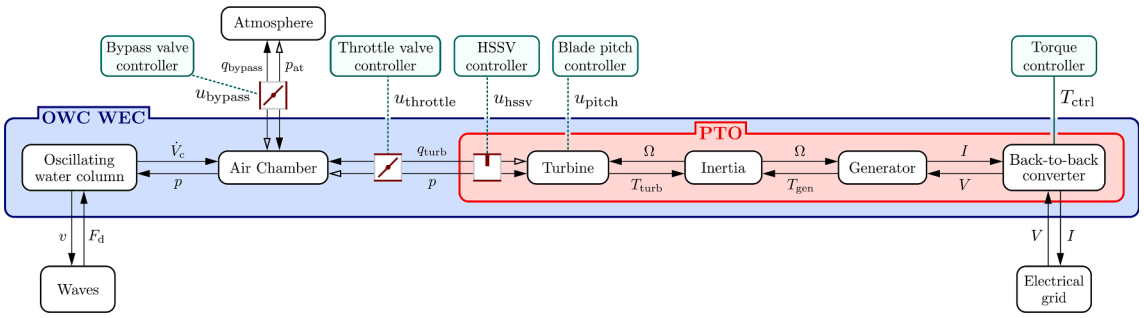

Fig. 3. Wave-to-wire power flow on an OWC wave energy converter. The bidirectional power flow between the air chamber, the turbine and the atmosphere is represented by double arrows. In the figure, V and I stand for voltage and electrical current, respectively. The bypass, throttle and HSSV valves are optional in an OWC WEC. The possibility of installing a blade pitch mechanism is also turbine type dependent. All variables are defined in the Nomenclature, and also in Section 3.

of air compressibility in the pneumatic chamber reduces structural stresses and fatigue problems. Therefore, air compressibility improves system reliability and reduces operational costs. However, air compressibility also changes the phase response of the OWC and may significantly impact the control design, especially in phase matching control strategies.

Another advantage of OWCs is the possibility to implement peak-shaving control [28] using a valve installed in series with the turbine (Section 5.4) which broadens the range of sea states over which power production can be maintained. A less effective alternative to peak-shaving control is the use of a bypass valve installed in parallel with the turbine [29,30] limiting the available pneumatic power. Limiting the impact of hydrodynamic power is a problem for many WEC types, often requiring the device to prematurely go into safe survival mode suspending power production.

Arguably, the biggest drawback of OWCs is the relatively high structural cost (which increases the LCoE). In addition, reactive control strategies, where power is injected into the system, are difficult to implement, since self-rectifying air turbines do not work efficiently as compressors [31].

3. Modelling OWC WECs

Fig. 3 shows the schematic of the power flow of an OWC, the green rectangles representing control inputs that may be used in a control strategy. Fig. 3 also shows the typical components of an OWC WEC and the physical variables involved at each step of the energy conversion chain. In this paper, for the sake of simplicity and clarity, we focus on fixed OWCs only.

3.1. Air chamber model

3.1.1. Time-domain air chamber model

Considering a fixed OWC, Fig. 1, a mass balance in the air chamber results in:

$$\frac{\mathrm{d}(\rho_c V_c)}{\mathrm{d}t} = -w_{turb} - w_{bypass}, \tag{2}$$

where ρ_c is the air density in the chamber, $V_c = V_0 - Sz$ is the instantaneous air chamber volume, V_0 is the chamber volume in still water conditions, S is the waterplane area of the water column, z is the OWC free surface vertical position (positive upward), w_{turb} and w_{bypass} are the turbine and bypass valve mass flow rates (both at inlet conditions and positive for outflow), respectively. Computation of the turbine mass flow rate is addressed in Section 3.4.1. The bypass valve mass flow rate is a function of the chamber pressure p_c, and the relative valve opening $0 \leqslant u_{bypass} \leqslant 1$, such that

$$w_{bypass}(p_c, u_{bypass}) = \mathrm{sign}(p_c) C_d(u_{bypass}) A_v \sqrt{2\rho_{in}|p_c|}, \tag{3}$$

where $C_d(u_{bypass})$ is the discharge coefficient, expressed as a function of u_{bypass}, where A_v is the valve area and 'sign' denotes the signum function. The stagnation air density, at the valve inlet, is given by:

$$\rho_{in} = \max(\rho_c, \rho_{at}), \tag{4}$$

where ρ_{at} and ρ_c are, respectively, the atmospheric air density and the instantaneous air chamber density, computed from the isentropic relation $\rho_c = \rho_{at}(p_c/p_{at})^{1/\gamma}$. The bypass valve volumetric flow rate is computed as $q_{bypass} = w_{bypass}/\rho_{in}$. Assuming that the air behaves as an ideal gas, and the compression/expansion process within the chamber can be modelled as an isentropic process, Eq. (2) can be written [32] as:

$$\frac{\dot{p}_c}{p_c + p_{at}} = -\gamma\left(\frac{\dot{V}_c}{V_c} + \frac{w_{turb} + w_{bypass}}{m_c}\right). \tag{5}$$

where p_{at} is atmospheric pressure, $\gamma = 1.4$ is the specific heat ratio, and $m_c = \rho_c V_c$ is the instantaneous air mass inside the chamber.

3.1.2. Frequency-domain air chamber model

Eq. (5) is valid in the time domain. To apply a frequency domain formulation, Eq. (5) needs to be linearised, considering the following approximations: (i) the pressure fluctuation p_c inside the air chamber is negligible, compared to atmospheric pressure, i.e. $p_c + p_{at} \approx p_{at}$; (ii) the chamber air density is approximately equal to atmospheric air density $\rho_c \approx \rho_{at}$; (iii) chamber volume fluctuations are small and the instantaneous air chamber volume is approximately equal to the volume in hydrostatic conditions $V_c \approx V_0$; (iv) the bypass valve requires a non-linear controller and cannot be included in the frequency domain, with the consequent frequency-domain assumption that $w_{bypass} = 0$; and (v) the turbine mass flow rate is linearly related to the relative air chamber pressure:

$$p_c = \kappa_{turb} w_{turb}, \tag{6}$$

where κ_{turb} is the turbine damping, further discussed in Section 3.4.1. Following the set of frequency-domain assumptions, linearisation of Eq. (2) yields:

$$\frac{V_0}{\gamma p_{at}}\dot{p}_c + \frac{p_c}{\rho_{at}\kappa_{turb}} = -\dot{V}_c. \tag{7}$$

The air volume displaced by the OWC ($\dot{V}_c$) is computed from the hydrodynamic model, as shown in Eqs. (9) or (10).

3.2. Hydrodynamic modelling in the frequency domain

OWC hydrodynamic modelling is traditionally carried out under the typical assumptions of the linear wave theory, or linear potential theory (LPT), first developed by Airy [33]. LPT assumes that the flow is incompressible and irrotational, and wave amplitudes and device

displacements are small compared to wavelength. Therefore, the potential flow can be described by the Laplace equation, since a velocity potential exists. Usually, OWCs are modelled using two related approaches: the piston model and the uniform pressure model, Fig. 4.

3.2.1. Piston model

In the oscillating body (referred to the water column) model, first proposed by Evans [34], the free surface of the water column is treated as a neutrally buoyant piston, characterised by its frequency dependant parameters: added mass $A(\omega)$, radiation damping $B(\omega)$, and excitation force $F_d(\omega)$. The frequency dependant parameters of the heaving oscillating plate can be computed experimentally [35] or numerically using boundary element method solvers for oscillating bodies such as WAMIT, NEMOH, AQWA, and others. This approach may be acceptable if the characteristic length of the OWC free surface is much smaller than the wavelength of the incident waves, and smaller than the length of the OWC. The equation of motion of the water column, subjected to harmonic excitation at frequency ω, may be written, in the frequency domain, [36] as:

$$\left(i\left(\omega\left(m_p + A\left(\omega\right)\right) - C_h\omega^{-1}\right) + B\left(\omega\right)\right)\widehat{v} = -S\widehat{p}_c + F_d\left(\omega\right), \tag{8}$$

where i is the imaginary unit, m_p is the piston mass, $C_h = \rho_w g S$ denotes the hydrostatic stiffness, ρ_w is the water density, g is the gravity constant, $\widehat{v}$ and $\widehat{p}_c$ are the complex amplitudes of the OWC free surface velocity and the relative pressure amplitude, respectively, such that $v = \widehat{v}e^{i\omega t}$ and $p_c = \widehat{p}_c e^{i\omega t}$. The displaced volume flow rate for the piston model is:

$$-\dot{V}_c = S\widehat{v}e^{i\omega t}. \tag{9}$$

The complex amplitudes of the velocity and pressure are computed by solving the system of Eqs. (7) and (8).

3.2.2. Uniform pressure model

The uniform pressure approach, introduced in [37], is more realistic and straightforward. This model assumes a uniformly distributed pressure on the inner free surface and, consequently, the free surface can deform. In this approach, the displaced volume flow rate is decomposed into an excitation flow rate, q_e, and radiated flow rate, q_r:

$$-\dot{V}_c = q_e\left(t\right) + q_r\left(t\right). \tag{10}$$

The excitation flow rate is exclusively due to incident waves, when $p_c = 0$. The radiated flow rate results from oscillations in air pressure inside the pneumatic chamber. A full treatment of the uniform pressure model, also known as the admittance approach, is found in [38].

If incident waves are regular waves of frequency ω, Eq. (10) may be rewritten, in the frequency domain, [39] as:

$$\widehat{q}_e + \widehat{q}_r = \left(i\frac{V_0}{\gamma p_{at}} + \frac{1}{\rho_{at}\kappa_{turb}}\right)\widehat{p}_c, \tag{11}$$

where $\widehat{q}_e$ and $\widehat{q}_r$ are the complex amplitudes of the excitation and radiated flow rates such that $q_e = \widehat{q}_e e^{i\omega t}$ and $q_r = \widehat{q}_r e^{i\omega t}$. The radiated flow rate can be decomposed in real and imaginary parts and written as a function of the relative pressure, giving $\widehat{q}_r = -(G(\omega) + iH(\omega))\widehat{p}_c$. The real-valued coefficients $G(\omega)$ and $H(\omega)$ are, respectively, the radiation conductance and radiation susceptance. The chamber pressure complex amplitude can be computed by substituting the definition of $\widehat{q}_r$ in Eq. (11) as:

$$\widehat{p}_c = \left(\frac{1}{\rho_{at}\kappa_{turb}} + G(\omega) + i\left(\frac{\omega V_0}{\gamma p_a} + H(\omega)\right)\right)^{-1}\widehat{q}_e. \tag{12}$$

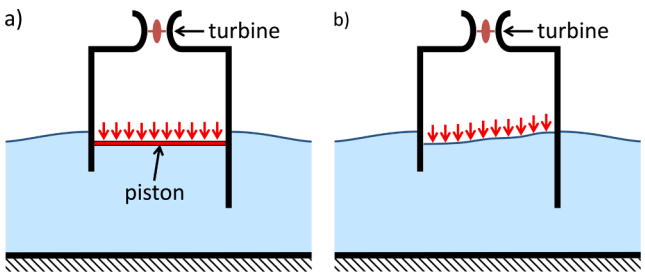

Fig. 4. a) Piston model versus b) uniform pressure free-surface model [9].

3.2.3. Relation between piston and uniform pressure models

The hydrodynamic coefficients of the massless disk approach, $A(\omega)$ and $B(\omega)$, and those of the admittance approach, $G(\omega)$ and $H(\omega)$, can be related [9] as follows:

$$\begin{aligned} \frac{S^2 G(\omega)}{G^2(\omega) + H^2(\omega)} &= B(\omega), \\ \frac{\omega S^2 H(\omega)}{G^2(\omega) + H^2(\omega)} &= -\omega^2\left(m_p + A(\omega)\right) + \rho g S. \end{aligned} \tag{13}$$

3.3. Hydrodynamic modelling in time domain

3.3.1. Piston model

The piston model in the time domain results in the classic Cummins' formulation

$$\begin{aligned} \left(m_p + A_\infty\right)\dot{v} &= -\rho_w g S z - S p_c + F_d - R, \\ \dot{z} &= v. \end{aligned} \tag{14}$$

The radiation damping force, F_r, is defined as $F_r = A_\infty \dot{v} + R$, where A_∞ represents the OWC added mass value at infinite frequency and

$$R = \int_{-\infty}^{t} K\left(t-\tau\right) v\left(\tau\right) \mathrm{d}\tau. \tag{15}$$

The kernel $K(\tau)$ is the piston impulse response function computed as the inverse Fourier transform of the radiation damping $B(\omega)$.

3.3.2. uniform pressure model

The radiation volumetric flow rate q_r is computed via the convolution integral:

$$q_r\left(t\right) = -\int_{-\infty}^{t} h_r(t-\tau) p_c(\tau) \mathrm{d}\tau, \tag{16}$$

resulting from the memory function $h_r(t)$ computed as the inverse Fourier transform of $G(\omega)$ through

$$h_r(s) = \frac{2}{\pi}\int_0^\infty G\left(\omega\right)\cos(\omega s)\mathrm{d}\omega. \tag{17}$$

3.4. Turbine/generator set modelling

The turbine/generator set dynamics can be modelled using either torque or power formulations, which have a direct equivalence. Using the power formulation:

$$\frac{\mathrm{d}}{\mathrm{d}t}\left(\frac{1}{2}I\Omega^2\right) = P_{turb} - T_{ctrl}\Omega, \tag{18}$$

where Ω, I, and P_{turb} are the turbine/generator set rotational speed, moment of inertia, and the turbine power, respectively. The instantaneous generator electromagnetic torque, T_{ctrl}, is a control input set by the power plant controller.

3.4.1. Air turbine modelling

For large Reynolds numbers and negligible compressibility effects on the turbine blades related to the Mach number, Buckingham's theorem [40] describes the dynamics of an air turbine using the dimensionless

mass flow rate Φ, and the dimensionless turbine shaft power Π, defined as

$$\Phi = \frac{w_{\text{turb}}}{\rho_{\text{in}} \Omega d^3}, \tag{19}$$

$$\Pi = \frac{P_{\text{turb}}}{\rho_{\text{in}} \Omega^3 d^5}, \tag{20}$$

where d is the turbine rotor diameter. Φ and Π are obtained experimentally and can be expressed, respectively, as:

$$\Phi = f_\Phi\left(\Psi, u_{\text{hssv}}, u_{\text{pitch}}\right), \tag{21}$$

$$\Pi = f_\Pi\left(\Psi, u_{\text{hssv}}, u_{\text{pitch}}\right), \tag{22}$$

where Ψ is the dimensionless pressure head,

$$\Psi = \frac{p_{\text{c}}}{\rho_{\text{in}} \Omega^2 d^2}, \tag{23}$$

and the control variables $0 \leqslant u_{\text{hssv}} \leqslant 1$ and u_{pitch} are, respectively, the relative opening of the high-speed stop valve (HSSV) and the pitch angle of rotor/stator blades. Since many OWCs do not have HSSVs and are equipped with fixed-pitch turbines, u_{hssv} and u_{pitch} do not always appear in the turbine model. If used, u_{hssv} and u_{pitch} represent additional (to T_{ctrl}) control inputs to the system.

The turbine aerodynamic power is computed using Eq. (22), as:

$$P_{\text{turb}} = \rho_{\text{in}} \Omega^3 d^5 f_\Pi\left(\Psi, u_{\text{hssv}}, u_{\text{pitch}}\right). \tag{24}$$

The turbine efficiency can be defined as

$$\eta_{\text{turb}} = \frac{P_{\text{turb}}}{P_{\text{pneu}}} = \frac{\Pi}{\Psi \Phi} = \frac{f_\Pi\left(\Psi, u_{\text{hssv}}, u_{\text{pitch}}\right)}{\Psi f_\Phi\left(\Psi, u_{\text{hssv}}, u_{\text{pitch}}\right)}, \tag{25}$$

where $P_{\text{pneu}} = p_{\text{c}}\, q_{\text{turb}}$ is the available pneumatic power and $q_{\text{turb}} = w_{\text{turb}} / \rho_{\text{in}}$ is the turbine volumetric flow rate.

Several studies use a set of dimensionless numbers proposed by Maeda et al. [41]. However, this set of dimensionless numbers were defined for incompressible flow and cannot be applied directly to a numerical model that considers the spring-like air compressibility effect of Eq. (5). Furthermore, Maeda's et al. approach does not follow the well-known Buckingham Π theorem [40]. The best approach is to convert Maeda's et al. dimensionless numbers to the set of dimensionless numbers described by Eqs. (19), (20) and (23); see B.

3.4.2. Electric generator modelling

The majority of OWC PTO systems do not operate at constant rotational speed. The doubly fed induction generator (DFIG), controlled by a B2B converter, represents a possible solution to operate OWC PTOs with variable rotational speed. The dynamics of a DFIG is described by four differential equations in terms of flux components. Two reference frames, for stator and rotor variables, rotating at synchronous speed, are considered [42]:

$$\begin{aligned}
\dot{\psi}_{\text{ds}} &= V_{\text{ds}} - R_{\text{s}} i_{\text{ds}} + \omega_{\text{s}} \psi_{\text{qs}}, \\
\dot{\psi}_{\text{qs}} &= V_{\text{qs}} - R_{\text{s}} i_{\text{qs}} - \omega_{\text{s}} \psi_{\text{ds}}, \\
\dot{\psi}_{\text{dr}} &= V_{\text{dr}} - R_{\text{r}} i_{\text{dr}} + \left(\omega_{\text{s}} - n_p \Omega\right) \psi_{\text{qr}}, \\
\dot{\psi}_{\text{qr}} &= V_{\text{qr}} - R_{\text{r}} i_{\text{qr}} - \left(\omega_{\text{s}} - n_p \Omega\right) \psi_{\text{dr}}.
\end{aligned} \tag{26}$$

The dynamic model is closed with the following algebraic relations:

$$\begin{aligned}
\psi_{\text{ds}} &= L_{\text{s}} i_{\text{ds}} + L_{\text{m}} i_{\text{dr}}, \\
\psi_{\text{qs}} &= L_{\text{s}} i_{\text{qs}} + L_{\text{m}} i_{\text{qr}}, \\
\psi_{\text{dr}} &= L_{\text{r}} i_{\text{dr}} + L_{\text{m}} i_{\text{ds}}, \\
\psi_{\text{qr}} &= L_{\text{r}} i_{\text{qr}} + L_{\text{m}} i_{\text{qs}}.
\end{aligned} \tag{27}$$

The terms $\dot{\psi}_{\text{ds}}, \dot{\psi}_{\text{qs}}, \dot{\psi}_{\text{dr}}$ and $\dot{\psi}_{\text{qr}}$ indicate the direct (d) and quadrature (q) flux components for rotor (r) and stator (s). The current (and voltage) components are $i_{\text{ds}}, i_{\text{qs}}, i_{\text{dr}}$ and i_{qr} (and $V_{\text{ds}}, V_{\text{qs}}, V_{\text{dr}}$ and V_{qr}). R_{s}, and R_{r} are, respectively, the electrical resistance for stator and rotor, while L_{s} and L_{r} are, respectively, the self-inductance of stator and rotor, with a mutual inductance between stator and rotor windings of L_{m}. Finally, with f_{s} denoting the grid frequency, $\omega_{\text{s}} = 2\pi f_{\text{s}}$ is the machine synchronous frequency and n_{p} is the number of pole pairs. The dynamic model of a permanent magnet synchronous generator (PMSG) can be found in [43].

3.5. Alternative modelling approaches: data-based modelling

System identification (SI), or data-based modelling, techniques [44] represent an alternative strategy to provide a hydrodynamic model for OWCs [45,46], compared to physics-based models (Sections 3.2 and 3.3). Despite being only recently applied to wave energy, SI has already been successfully employed in WEC modelling. With SI, the model parameters are derived from input/output data by minimising a model-related cost function. Once the model parameters are identified, the parametric model has to be validated against a separate set of data. SI models can be solely based on data (black-box models), or can take into account, to varying extents, some physics-based information (grey-box models) [47].

Data-based models can be linear or nonlinear, depending on the specific parameterisation [48]. Nonlinear models can have more accurate and broader validity, while the simplicity of linear models, including their suitability as a platform for model-based control, is appealing. One advantage of linear data-based WEC models is that they can be more representative of a wider operational range [49] than those developed from first principles, which assume infinitesimally small variations around an equilibrium point (usually the still water level), depending on the range of the data employed to identify the model. This can help to overcome the so-called *modelling paradox* [50] for WECs, where models developed under the assumption of small variations are subsequently employed for WEC control design, which generally try to exaggerate the WEC motion and therefore violate the small-variation assumption. However, care must be taken in the choice of excitation for the WEC, so that suitable identification data is obtained, with reference to the model purpose and range of validity [51].

4. Operation of power take-off components

This section examines the principal PTO components (air turbine and generator) and focuses on their operational characteristics and their facility as control elements.

4.1. Wells turbine

The Wells turbine rotor consists of a set of uncambered blades, symmetrically positioned about a plane normal to the rotational axis, Fig. 5 a) and b) [52]. This configuration produces a unidirectional time-averaged torque from a bidirectional air flow without the need for rectifying valves. Rotational speed control in Wells turbines has two primary goals: i) operate the turbine close to the best efficiency point, and ii) avoid aerodynamic stall on turbine blades that occurs for values of Ψ above a critical value Ψ_{crit}, Fig. 6 a). The operational range of high-efficiency Wells turbines is narrow, Fig. 6 b), compared with impulse turbines, Section 4.2. The sharp drop in the efficiency of the Wells turbine is a consequence of blade stall that develops when the angle of attack of the rotor blades increases with the flow rate, Fig. 5 b).

The hard-stall characteristics of the Wells turbine blades introduce an aerodynamic constraint to all control strategies. To avoid stall for large pressure heads p_{c}, Ω must increase such that the condition $\Psi < \Psi_{\text{crit}}$ is always verified. Therefore, the rotational speed must be greater than $\Omega \geqslant \sqrt{\left|p_{\text{c}}\right| / \left(\rho_{\text{in}} \Psi_{\text{crit}} d^2\right)}$. This implies that large pressure heads require high rotational speeds. However, Ω is limited to: i) shock wave occurrence on the blades suction surface [53], and ii) blade stresses that result

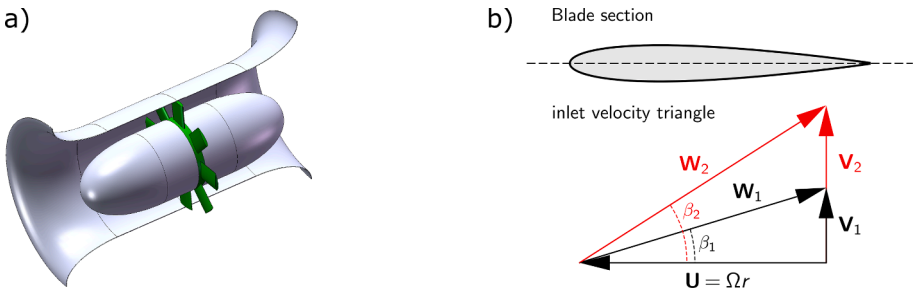

Fig. 5. a) A Wells turbine without guide vanes. b) A typical aerofoil section of a rotor blade and the inlet velocity triangles for two flow rates.

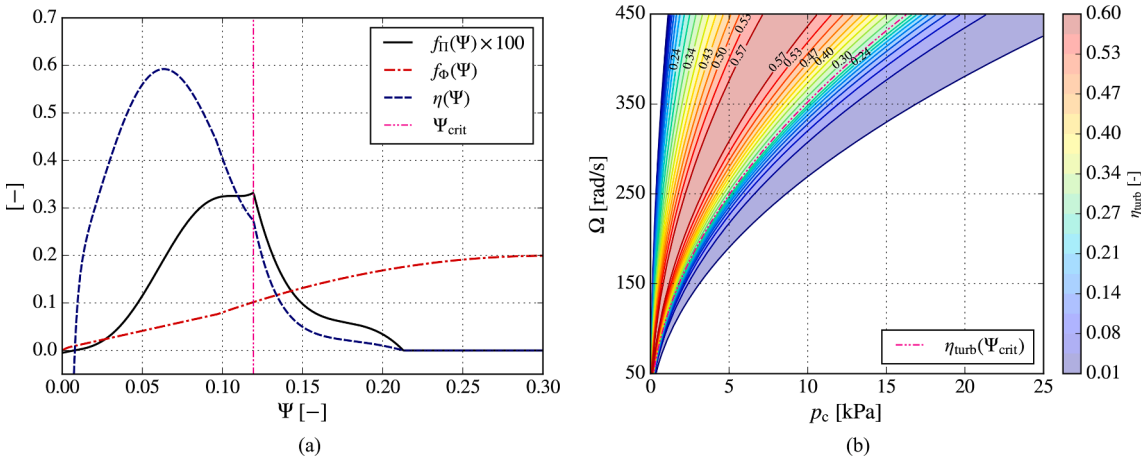

Fig. 6. a) Efficiency of the Wells turbine installed at the Mutriku wave power plant as a function of the dimensionless pressure head. b) Mutriku's Wells turbine efficiency map as a function of the pressure head p_c and the rotational speed Ω for a turbine diameter of $d = 0.75$m. The white regions represents areas of zero or negative efficiencies.

from the centrifugal forces, which increases with Ω^2. The blade tip speed velocity is usually limited to $v_{tip} = \Omega d/2 \leqslant 180$,m/s to avoid shock waves [10]. Well designed Wells control algorithms try to avoid stall by increasing rotational speed while not exceeding blade tip speed limit and maximum allowed mechanical stresses. Another side effect of aerodynamic turbine blade stall, and shock waves, is significantly increased noise emissions [54]. Fig. 7.

The Wells turbine efficiency characteristic, up to the best efficiency point, shows a linear relation between the dimensionless flow rate and the dimensionless pressure

$$\Phi = k_w \Psi, \tag{28}$$

where k_w is a constant that depends on the turbine geometry but not on its size, resulting in

$$w_{turb} = \frac{k_w d}{\Omega} p_c. \tag{29}$$

Eq. (29) shows that the Wells turbine rotational speed control affects the flow rate. This interaction between the instantaneous rotational speed and the hydrodynamics needs to be considered when designing an efficient controller. Additionally, OWCs with Wells turbines should have a safety valve installed in the turbine duct to control excessive centrifugal stresses resulting from the high runaway speed achieved if the electrical generator torque vanishes. A high-level safety controller should close the safety valve in case of an electrical equipment malfunction or a connection failure to the electrical grid.

Finally, to delay stall and improve Wells turbine performance under stall conditions, a passive flow control technique based on multiple suction slots on the rotor blades is investigated in [55,56].

4.2. Impulse turbines

4.2.1. Axial-flow impulse turbines

Axial-flow impulse turbines have rows of stator guide vanes, before

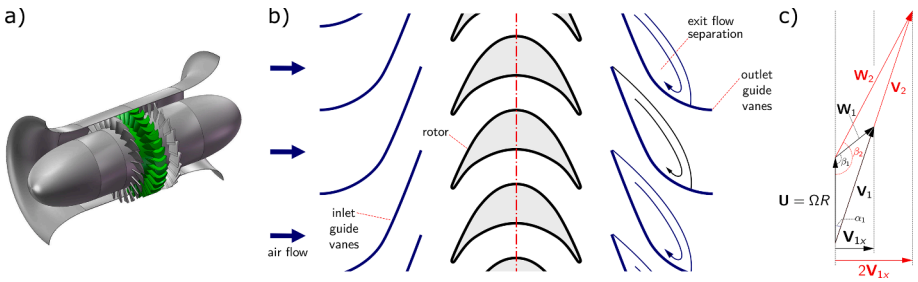

Fig. 7. a) An axial-flow impulse turbine. b) A typical rotor cascade with guide vanes. c) Rotor inlet velocity triangles for two flow rates. The quantities $\mathbf{W}, \mathbf{U}$, and $\mathbf{V}$ are, respectively, the relative, the transport, and the absolute velocities. In this figure only, R refers to the rotor blade radius.

(upstream) and after (downstream) the turbine rotor, to operate effectively with a bidirectional air flow [57]. The upstream stator guide vanes are required to increase the air flow kinetic energy by reducing the air pressure. The air flow exits the rotor with reduced swirl and the downstream row of guide vanes behaves as a partial flow blockage, significantly reducing the turbine efficiency. To reduce these losses, a possible solution is having guide vanes with variable pitch angle [58,57].

In the standard configuration, axial-flow impulse turbines are installed in a duct with a constant radius cross-section. This arrangement presents peak efficiencies significantly lower than the Wells turbine, although they do not show the sharp efficiency drop characteristic of Wells turbines. The Voight company proposed an axial rotor impulse turbine called HydroAir [59] where the upstream and downstream rows of guides vanes are installed in a conical duct at a larger radius, to decrease the losses at the exit stator vanes. The idea is to reduce the axial and tangential velocities, as a consequence of the duct area increase and the conservation of angular momentum.

An ideal impulse turbine shows a relationship between Φ and Ψ of the form

$$\Phi = \mathrm{sgn}\left(\Psi\right) k_\mathrm{i} \sqrt{|\Psi|}, \tag{30}$$

where k_i is a constant that depends on the turbine geometry but not on its size, resulting in

$$w_\mathrm{turb} = \mathrm{sgn}\left(p_\mathrm{c}\right) k_\mathrm{i} d^2 \sqrt{\rho_\mathrm{in} |p_\mathrm{c}|}. \tag{31}$$

Eq. (31) shows that ideal turbine damping is not affected by control of the rotational speed. It also shows that the coupling between the hydrodynamics and the turbine is only a function of the pressure, if the air compression/expansion process is assumed to be isentropic. The comparison between Figs. 6 b) and 9 b) shows that rotational speed control of impulse turbines is simpler due to their broader operational range.

4.2.2. Radial-flow impulse turbines

A radial impulse turbine was proposed by McCormick et al. [60] and optimised in [61]. This turbine configuration is not symmetrical and shows an efficiency that depends on the radial-flow direction. Moreover, the peak efficiency of this turbine is penalised by the exit stator vanes, as in axial-flow turbines.

A different idea was proposed by Falcão and Gato as the biradial turbine [62], Fig. 8. The biradial turbine is symmetrical to a plane perpendicular to the axis of rotation, with the rotor inflow radial centripetal, while the outflow is radial centrifugal. The aerodynamic losses of this turbine are much lower than other impulse turbines for three reasons: i) flow is highly decelerated in the diffuser before entering the radially offset exit guide-vane row (losses $\propto v^2$); ii) the stator has two rows of concentric guide vanes [63]; and iii) deflection of flow from radial centripetal to radial centrifugal occurs inside the rotor. Foe these reasons, the biradial turbine has the highest peak efficiency, Fig. 9 a), and a much wider operating range (Fig. 9 b)) than the Wells turbine.

Since radial-flow impulse turbines (Fig. 8) have narrow inlet/outlet ducts, the air flow can be easily controlled with relatively small and fast control valves, which can be used for different purposes (e.g., latching and peak-shaving control). The first turbine that successfully tested a HSSV was the biradial turbine at the Mutriku wave power plant [28].

4.3. Variable-pitch turbines

Variable-pitch turbines offer an additional degree of freedom which can be potentially exploited to optimise performance. In [64], a design for a 400 kW variable-pitch turbine for the Pico power plant is described. Despite the fact that pitch control is very popular in wind energy applications, this solution is not widely employed in OWCs due to their complexity, cost, and possible reliability issues related to the continuous operation of the pitch actuation mechanism. Investigation into the effect of variable pitch on air turbines for OWCs can be found in [65,66].

The Denniss-Auld turbine is a self-rectifying axial-flow turbine with some characteristics in common with variable-pitch turbines [67]. The rotor blades of this turbine are symmetrical with respect to the mid-chord plan, perpendicular the rotational axis (similar to the impulse turbine rotor). Guide vanes are avoided by pitching (almost instantaneously) the rotor blades between their extreme positions.

In axial-flow impulse turbines, variable-pitch guide vanes mainly aim to reduce the aerodynamic losses due to the blockage effect of the second row of guide vanes [58,57]. To avoid a complex active actuation system, the guide vanes may autonomously/passively pivot under the effects of aerodynamic moments.

4.4. Unidirectional air turbines

OWC devices can be equipped with unidirectional air turbines, although an air rectifying system is needed for this configuration. Air rectification is typically achieved using one-way pressure-driven control valves, which automatically (or passively) open/close, depending on the pressure in the pneumatic chamber. Modelling of air rectifying systems for OWC WECs is addressed, for instance, in [36,68]. Furthermore, a unidirectional air turbine, for a fully-submerged bottom-standing WEC equipped with rectifying valves, is tested in [69,70].

4.5. Electrical generator

The typical rotational speed range for self-rectifying air turbines permits the turbine to be directly coupled with the generator without need for a mechanically complicated and potentially expensive gearbox. In [18], the problem of generator selection for offshore OWCs is addressed. The authors compare different possible variable speed generators in terms of suitability for wave energy, cost, durability/maintenance, efficiency, and grid integration aspects. Ultimately, PMSGs seem to be the best (but expensive) option, although DFIGs have also proven to be suitable for wave energy applications.

A control law should consider the performance characteristics of the generator, to maximise the electrical power delivered to the grid. Fig. 10 shows the efficiency map for a typical DFIG generator as a function of Ω and T_ctrl. The map shows that the generator has relatively low efficiency, for low Ω and T_ctrl. Therefore, selecting a generator with a rated power much lower than the expected annual-averaged turbine power output reduces the energy delivered to the grid. Plotted in Fig. 10 are three possible generator operating curves, revealing that the overall

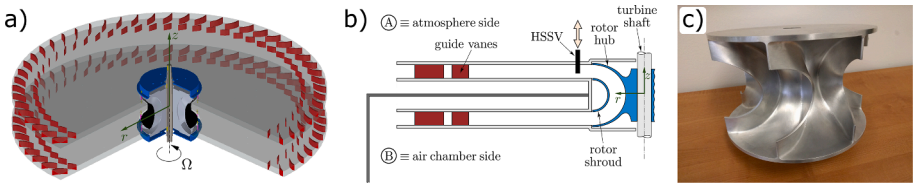

Fig. 8. a) Biradial turbine with two rows of fixed guide-vanes radially offset from the rotor. b) Cut of the turbine showing the position of the sliding HSSV. c) Picture of a small-scale rotor with a diameter of 0.25 m.

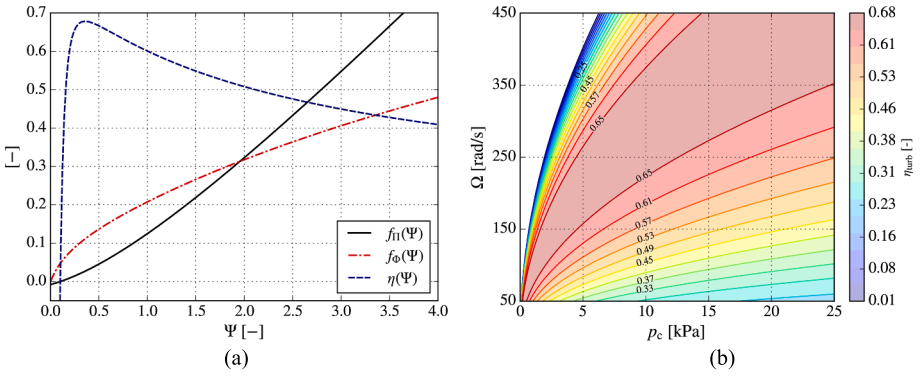

Fig. 9. a) Biradial turbine efficiency as a function of the dimensionless pressure head. b) Biradial turbine efficiency map as a function of the pressure head p_c and the rotational speed Ω for a turbine diameter of $d = 0.5$m. The white region represents areas of negative efficiencies.

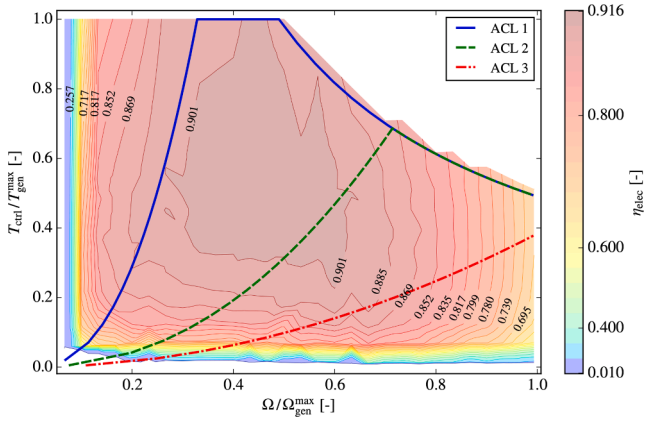

Fig. 10. Generator efficiency map measured at the IST laboratory in steady conditions [71].

performance depends on the selected control path (Section 5.1.2).

5. Review of current control strategies

Controllers manipulate and synchronise the control inputs to achieve predefined goals, with the maximisation of the time-averaged turbine power output the most common goal. As show in Fig. 3, and described in Section 3, controllers for OWC WECs typically use the following manipulated inputs:

- Generator electromagnetic torque, T_{ctrl},
- blade pitch position, u_{pitch},
- bypass valve position, u_{bypass},
- HSSV position, u_{hssv}, and
- throttle valve position, $u_{throttle}$.

Since the OWC control problem depends heavily on the device components (both system and available actuators), we propose a broad classification of control strategies based on an *objective-focused* perspective. Therefore, it may be possible to distinguish between three main types of control objectives, namely turbine control, hydrodynamic control, and grid-side control.

Fully-rated bi-directional B2B power converters offer the possibility to naturally split the OWC control problem at the level of the-DC link [23] and, consequently, device-side control (i.e., turbine and hydrodynamic control) can be treated independently from grid-side control.

In relation to device-side control, if available wave power is relatively high, the electric generator could potentially attain its rated power. To keep the generator working at its rated power, the OWC system must dissipate excessive power; otherwise, the device must be shut down to avoid major failures. Therefore, power dissipation control becomes necessary.

5.1. Turbine control

In general, the aim of turbine control is to keep the turbine around its maximum efficiency point and, consequently, to optimise the pneumatic-to-mechanical energy conversion process. Rotational speed control is more straightforward in impulse turbines than in Wells turbines, since rotational speed does not affect turbine damping in impulse turbines, Eq. (31). As such, impulse turbine control is a relatively simple setpoint following control problem for turbine rotational speed, as a function of the pressure head [72]. For Wells turbines, though the mass flow rate depends on the rotational speed, Eq. (29), hydrodynamic/aerodynamic interaction is typically neglected, with a resulting simplification to a setpoint following problem. It should be noted that Wells turbine control can potentially improve the hydrodynamic response of OWCs by optimising instantaneous turbine damping. However, to the best of the authors' knowledge, combined hydrodynamic/aerodynamic control, through turbine rotational speed modulation, has never been attempted. The setpoint following problem can be further divided into a rotational speed setpoint determination problem (Section 5.1.1 and a rotational speed tracking problem (Section 5.1.3).

Turbine rotational speed can be controlled by the generator torque and/or through valves in series, or in parallel, with the turbine. In the literature, alternative names to rotational speed control are sometimes employed, such as flow control (when valves are used), or torque control. To keep turbine operating in the high-efficiency region (see Figs. 6b)), aerodynamic stall should be avoided, since it leads to poor turbine performance. Due to its hard aerodynamic stall characteristic and relatively narrow peak efficiency region, rotational speed control is more challenging for a Wells turbine than for an impulse-like turbine. From a control perspective, turbine stall is due to incorrect determination of the rotational speed setpoint (e.g., as a result of sensors fault), or poor rotational speed tracking performance, which is primarily influenced by the inertia of the turbine/generator set. Inertia-related issues are further discussed in Section 5.1.3. Finally, from an electrical power quality perspective, the control algorithm should take advantage of the kinetic rotational energy stored by the flywheel, meaning that the conversion of mechanical to electrical power by the generator does not need to follow instantaneous turbine power.

5.1.1. Rotational speed setpoint determination

To optimise the pneumatic-to-mechanical energy conversion process, the turbine should be kept around its best efficiency point (BEP). The turbine BEP is an operating point at a fixed Ψ (see, for instance, Fig. 6), denoted as Ψ_{bep}. Since Ψ_{bep} is unique, for a given instantaneous relative air chamber pressure p_c, the instantaneous rotational speed that

maximises the turbine efficiency is given (Eq. (23)) by

$$\Omega_{\text{bep}} = \sqrt{\frac{|p_c|}{\rho_{\text{in}} d^2 \Psi_{\text{bep}}}}. \tag{32}$$

The main issue, associated with tracking the desired rotational speed Ω_{bep}, is the large torque variation usually required by most controllers, due to significant inertia of the rotating parts, and the large fluctuations of the relative air chamber pressure within each pseudo half-wave cycle. Furthermore, Eq. (32) shows that, when p_c tends to zero, the optimal rotational speed drops to zero as well, but this behaviour is undesirable in practice because it negatively affects power supply quality. The available pneumatic power grows from zero to a maximum value during each pseudo half-wave cycle and, to improve the pneumatic-to-mechanical energy conversion process, turbine efficiency should be kept at its highest value when the pneumatic power is maximal. A less important issue concerns turbine operation at low efficiency, when pneumatic power is relatively small.

In addition to the formulation of Ω_{bep}, Eq. (32), the value of Ω_{bep} can also be calculated from the mean axial-flow speed, $\bar{v}_x$. Fig. 11, taken from [73], shows the optimum control torque that has to be applied to follow Ω_{bep}. However, it is practically impossible to directly measure the mean axial velocity $\bar{v}_x$ in real-time and, hence, $\bar{v}_x$ is estimated based on the mean flow rate $Q = \bar{v}_x A$, computed using the relative chamber pressure p_c. At the BEP, the flow rate coefficient is $\Phi_{\text{bep}} = Q/\left(\Omega d^3\right)$, giving $\bar{v}_x = \left(\Phi_{\text{bep}} A/d^3\right)\Omega = \text{const} \times \Omega$.

It should be noted that the desired reference rotational speed, Ω_{ref}, may differ significantly from Ω_{bep}. For instance, in [74], two different reference rotational speeds (which, in this specific case, are tracked with a proportional (P) torque controller) are proposed for the Wells turbine mounted on one of the U-shaped OWCs of the breakwater of Civitavecchia (Italy). In the first case, the optimum speed is calculated as a function of the sea state only; hence, if the sea state is fixed, the optimum rotational speed is constant. A wave probe located at a suitable upwave location is used to record data for estimation of the sea state. The second strategy uses a varying reference rotational speed calculated from a maximum power point tracking (MPPT) algorithm for OWC turbines, based on Eq. (32).

Ultimately, turbine control approaches, based on a constant reference speed, can provide good performance, especially in relatively low energy sea states [75]. Furthermore, operating the turbine at a suitable constant reference speed may be convenient, particularly if turbines with a relatively high moment of inertia are used. However, if the constant reference speed depends on the sea conditions, the sea state has to be estimated using, typically, data collected from wave probes. As such, in addition to the increase in CapEx and OpEx due to the wave probes, if the sea state estimate is not accurate, the hypothetical controller (chosen for tracking the reference speed) will track an incorrect reference speed, potentially compromising the benefit of turbine control.

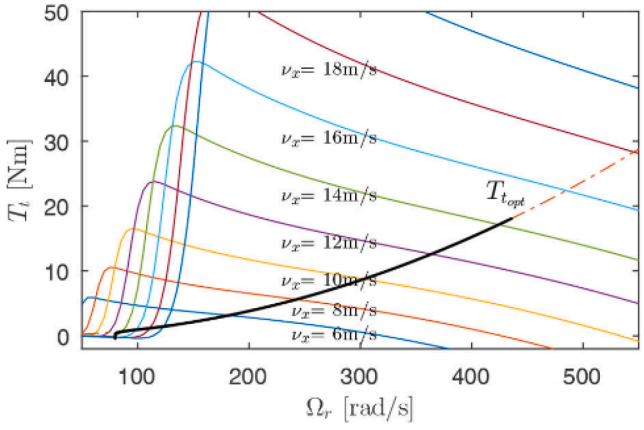

Fig. 11. Optimum control torque for optimising the turbine efficiency, T_{topt}, for different conditions of airflow speed, v_x. The coloured curves represent the values that T_t assumes for different values of the rotational speed, Ω_r, when v_x is fixed. Figure taken from [73].

5.1.2. Algebraic control law

A possible rotational speed control algorithm was introduced in [76] for Wells turbines. The algorithm aims to reach Ω_{bep} indirectly and can be derived from simple physical arguments, as follows: at the maximum turbine efficiency point, the turbine power output is given by

$$P_{\text{turb}}^{\text{bep}} = \rho_{\text{in}} \Omega^3 d^5 \Pi\left(\Psi_{\text{bep}}\right). \tag{33}$$

Since $\rho_{\text{in}} \approx \rho_{\text{at}}$, we find that $P_{\text{turb}}^{\text{bep}}$ should be proportional to Ω^3 and, therefore, we may impose a generator torque law of the type

$$T_{\text{ctrl}} = a\Omega^b, \tag{34}$$

where $a = \rho_{\text{at}} d^5 \Pi\left(\Psi_{\text{bep}}\right)$ and $b = 2$. In practice, the constants a and b of the algebraic control law (ACL) can be fine-tuned for a particular sea state or wave climate, and the specific turbine type. Unsurprisingly, ACL operates better in OWC WECs with relatively low PTO inertia and, correspondingly, faster dynamics, see Eq. (18). It should be noted that the ACL can be modified to avoid exceeding the generator rated power, $P_{\text{gen}}^{\text{rated}}$, and the maximum allowed torque, $T_{\text{gen}}^{\text{max}}$, using

$$T_{\text{ctrl}} = \min\left(a\Omega^b, \frac{P_{\text{gen}}^{\text{rated}}}{\Omega}, T_{\text{gen}}^{\text{max}}\right). \tag{35}$$

However, as shown in Fig. 12, T_{ctrl} calculated from Eq. (35) does not avoid turbine over-speeding. A possible solution to avoid turbine over-speeding is to use a generator with a maximum torque such that the probability of over-speeding is low, Fig. 12a). In this case, the generator torque increases to its maximum value when the rotational speed goes above a given threshold and then follows the maximum torque and maximum power constraints. However, the use of a supervisory HSSV controller can ensure that the maximum rotational speed is never exceeded [32]. In essence, when the maximum rotational speed is reached, the HSSV is first closed and then reopened when the rotational speed reduces below a given threshold. Fig. 12b)-d) show the three possible types of control laws that result from reaching three different constraints: Generator rated power, maximum torque and maximum rotational speed. In [32], the control law in Eq. (35) is numerically tested on a biradial turbine, as well as on one of the Wells turbines mounted on the Mutriku power plant.

5.1.3. Rotational speed tracking

When the desired rotational speed setpoint is determined, there are many possible controllers that can be employed to track the reference speed. For OWCs, the two currently most popular solutions are Proportional-Integral-Derivative (PID) controllers and sliding mode controllers, which have quite different characteristics, with the broad distinction of linear/nonlinear, respectively. Fig. 13.

Tracking of the instantaneous rotational speed is primarily influenced by the inertia of rotating parts: air turbine and generator rotors, plus the connecting shaft. Low-inertia turbines can be controlled to operate close to the BEP by applying relatively small torque commands. For instance, Ceballos et al. [77] numerically and experimentally tested two separate control strategies for a Wells turbine. In the first case, a Proportional-Integral (PI) torque controller is used to track the optimum turbine rotational speed (Eq. (32)), whereas the second strategy uses the ACL of Eq. (34). Two different inertia values were considered for comparison and, unsurprisingly, the low-inertia turbine case provides better performance, with an increase in the turbine power up to 13% (with the PI controller) and 9% (with the ACL) compared to the high-inertia

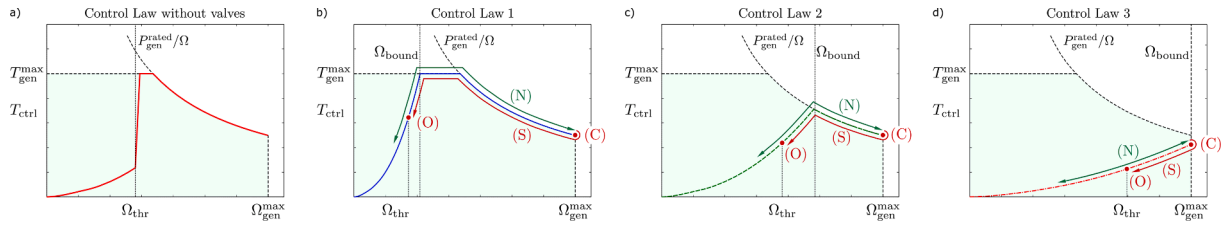

Fig. 12. The green shaded area represents the allowed operating region for the generator control laws as a function of the torque and rotational speed. The following notation was used: (N) normal operation, (C) close safety valve in series with the turbine, (S) safety mode (valve closed), and (O) open valve (resume to normal operation). Figure taken from [32].

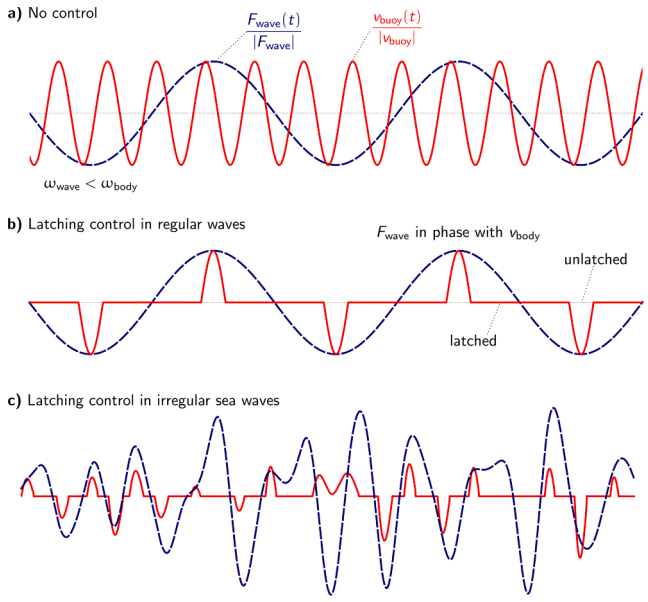

Fig. 13. a) Typical velocity for heaving buoy with a natural frequency higher than the frequency of the excitation force. b) Latching control to align the phases of the heave velocity and the excitation force. c) Latching control for a system subject to irregular sea waves. Figure taken from [106].

turbine. Even with a relatively high-inertia turbine, if enough torque variation is applied, it may be possible to track relatively fast variations in the reference rotational speed. However, since larger torque variations require a more powerful (and expensive) electric generator, there is a risk of ending up with an oversized generator, which may consequently have a relatively low capacity factor. Therefore, since the ultimate objective of control should be LCoE minimisation, increasing the size of the electric generator may not be a good solution since it may negatively impact the LCoE, particularly CapEx.

PID controllers. PID control is a well-known intuitive control technique for setpoint-following feedback loops. For that reason, PID control has been applied to a variety of OWC subsystems, including the primary function of rotational speed control and, at a lower level, servo control of generator torque or valve positions. Despite the fact that satisfactory performance may be achieved using PID control, PID controllers may not be the best solution for rotational speed control. Specifically, in comparison to other control techniques for setpoint-following feedback loops (for instance, sliding mode control), the main drawback of PID-based OWC control schemes is the relative lack of robustness.

Defining, $e(t)$, as the difference between the actual value of the variable to be tracked (e.g., electric generator currents) and the desired reference value of that variable, the control input provided by a PID is given by

$$u_{pid} = K_p e\left(t\right) + K_i \int_0^t e\left(\tau\right) d\tau + K_d \frac{de(t)}{dt}, \tag{36}$$

where K_p, K_i, and K_d are, respectively, the proportional, integral, and derivative gains of the PID controller.

In [78], two turbine control strategies, which rely on two different types of actuators to maximise turbine efficiency, are proposed for the Mutriku OWC plant and tested in both regular and irregular waves. The first strategy relies on a torque controller, while the second control approach uses a throttle valve controller. The generator control torque is regulated by means of a PI controller, whereas the throttle valve position is adjusted using a PID controller, whose gains are tuned with the closed-loop Ziegler-Nichols (ZN) method. Both control strategies increase the time-averaged electrical power, with the PI torque controller slightly superior to the PID throttle valve controller. To assess the value of a combined torque/valve control strategy, the torque controller is used in combination with the (throttle) valve controller in [79]. Ultimately, the combined torque/valve control strategy improves the averaged generator power, especially if compared to the performance obtained with the (PID) throttle valve controller alone. Arguably, the major benefit of the combined torque/valve control strategy is the more accurate control of the rotational speed, which leads to higher turbine average power, particularly in low energy sea states [79]. The combined torque/valve strategy proposed in [79] is also considered in [80] but, to improve the fault-ride-through capability of the control strategy, and avoid the need of a rotor speed sensor, a closed-loop observer is used to estimate the rotational speed.

In addition to papers [78–80], many other turbine control strategies with PID controllers can be found [81–88], where, the main difference is generally in the tuning method of the PID controller. For instance, some of the PID tuning algorithms/methods found in the literature are: Grouped grey wolf (GGW) optimisation [81], artificial neural network (ANN) [84,85,88], zero-pole cancellation (ZPC) [77,89], self-adaptive global-best harmony search (SGHS) [86], harmony search (HS) [83], particle swarm optimisation (PSO)[82], fractional PSO memetic (FPSOM)[82], and fuzzy gain scheduling (FGS) [83]. Typically, the best performance is obtained when the PID gains are adapted in real-time (for instance, with a FGS technique [83]), although the complexity of the tuning method increases significantly. Ultimately, even though the use of sophisticated tuning algorithms marginally improves the performance of the PID controller, simpler tuning methods, such as Ziegler-Nichols, can still provide satisfactory performance.

Sliding mode controllers. A possible nonlinear control approach for tracking the turbine rotational speed is sliding mode control (SMC) [90]. Sliding mode control is particularly appealing due to its capability of coping with unmodelled dynamics, system uncertainties, nonlinearities and external disturbances.

A sliding variable, σ, which is a function of the system states, is defined so that the control objectives are satisfied for $\sigma = \dot{\sigma} = 0$. The condition $\sigma = \dot{\sigma} = 0$ defines a sliding surface in the state space. For rotational speed control, the sliding variable may be defined as

$$\sigma = \Omega - \Omega_{ref}. \tag{37}$$

To derive the control law, the sliding variable is differentiated until the manipulated variable (e.g. quadrature voltage or quadrature current of the generator) explicitly appears. Regardless of the different control

design procedures, the control gains of the sliding mode controller are tuned to make the system converge, robustly and in a finite time, to the condition $\sigma = \dot{\sigma} = 0$.

Compared to the ACL, SMC may present higher peaks in the generator control torque when the turbine power reaches zero [75]. The presence of control torque peaks depends on how the SMC is tuned, as well as on torque limits with respect to the inertia of the rotating parts. In general, higher control torque peaks lead to a higher peak-to-average power ratio and to an inferior power quality.

In [91], performance of a SMC strategy for an array of three OWCs, each of them equipped with a biradial turbine coupled with a DFIG, are compared to the results provided by the ACL. Both ACL and SMC are able to provide similar performance. For a single OWC, in comparison to ACL, SMC provides a higher time-averaged generator efficiency (91.97% versus 84.65%), but a slightly lower time-averaged electrical power (6.24 kW versus 6.46 kW).

In [73], a second-order sliding mode control (SOSMC) approach is numerically tested for a Wells turbine coupled with a DFIG. The primary objective of the control strategy focuses on maximising the turbine power output and, to this end, a MPPT algorithm is used to determine the BEP of the turbine. The secondary objective of the control strategy aims to regulate the stator reactive power of the generator. A twisting algorithm (TA) and a super twisting algorithm (STA) are used, respectively, to accomplish the primary and secondary objectives of the control strategy. The main advantage of a SOSM approach over a first-order SMC scheme is chattering amelioration (reduction of high frequency oscillations of the manipulated variable), which leads to better power quality and smoother control action.

In [92,93], different rotational speed control strategies are designed for the Wells turbines mounted on the Mutriku power plant. In [92], a SMC strategy for the torque controller is employed. In comparison to the uncontrolled case, the time-averaged electrical power is increased (after reducing the chattering phenomenon) by 12.95% with SMC, whereas worse performance are found for the PI torque controller (a 7.12% improvement) considered in [82]. In [93] a FGS-SMC rotational speed control strategy is proposed. In comparison to traditional SMC, the produced power is increased by 19.33% with the FGS-SMC scheme and, moreover, the fluctuations of the generated power due to the chattering phenomenon are significantly reduced.

Model predictive control. Despite the fact that model predictive control (MPC), relatively popular for other WEC types [94], is not the most popular choice for OWC turbine control, some MPC strategies for OWC turbines can be found in the literature [95,96]. In general, MPC-based strategies can provide good tracking performance for a constant rotational speed reference [95], as well as for a time-varying reference speed value [96].

In comparison to PID control and SMC, the main advantages of MPC, in addition to working with multi-variable systems, is the possibility to naturally deal with physical constraints, which can be easily taken into account in the optimisation problem. Arguably, since MPC requires prediction, at each time step, of some specific future states of the system over a receding horizon, the main disadvantage of MPC is the relatively high computational cost. As such, MPC may be difficult to implement in real-time control applications due to the significant computational burden, especially if relatively long receding horizons are employed.

Other possibilities for rotational speed tracking. In addition to SMC, alternative nonlinear controllers, which are suitable for rotational speed control in OWCs, include backstepping (BS) [97,98] and fuzzy logic controllers (FLC) [99].

5.2. Hydrodynamic control

OWC hydrodynamic control aims to optimise the wave-to-pneumatic energy conversion process. OWC hydrodynamic control approaches may be divided into three main categories: reactive control (Section 5.2.1), latching control (Section 5.2.2), and declutching control (Section 5.2.3).

5.2.1. Reactive control

In the frequency domain, the conditions for optimal wave energy absorption can be written as an impedance matching problem [100]. Let $Z_{\mathrm{i}}(\omega)$ and $Z_{\mathrm{PTO}}(\omega)$ be, respectively, the intrinsic impedance of the considered WEC and the PTO impedance. The optimum PTO impedance, which maximises the maximum power transfer from the WEC to the PTO, can be written, as

$$Z_{\mathrm{PTO}}(\omega) = Z_{\mathrm{i}}^{*}(\omega), \tag{38}$$

where * denotes the complex conjugate. From the control formulation in Eq. (38), which is only valid at a single frequency (ω), a control structure, known as approximate complex conjugate, can be derived [101]. Some attempts to generalise Eq. (38) to multi-frequency case are reported, for instance, in [102].

For OWC devices, the condition in Eq. (38) can be also written in terms of an optimal pressure profile [38], as

$$\widehat{p}_{\mathrm{c}}\left(\omega\right) = \frac{\widehat{q}_{\mathrm{c}}(\omega)}{2G(\omega)}. \tag{39}$$

To achieve the condition in Eq. (39), which is a condition on the pressure complex amplitude, $\widehat{p}_{\mathrm{c}}$ should be in phase with $\widehat{q}_{\mathrm{c}}$. Since $G(\omega)\geqslant 0$, but $\widehat{p}_{\mathrm{c}}(\omega)$ and $\widehat{q}_{\mathrm{c}}(\omega)$ can have opposite signs, to apply reactive control or, in general, to fully control the overall device hydrodynamic impedance, the PTO should be able to *supply* power for some parts of the wave energy conversion cycle. In practice, the need for reactive power in power system (which is different from electrical reactive power [23] in electric generators) is somewhat difficult to provide. Indeed, the peak reactive power can be significant, PTO efficiency can differ in the direct and reverse operation modes, and losses are not expected to be negligible for a bi-directional power transfer process [103]. Furthermore, on OWC devices, reactive control is typically difficult to implement due to the nature of self-rectifying air turbines, which do not work efficiently as air compressors [31].

A few papers on reactive control for OWCs can be found. For instance, OWC reactive control with variable-pitch turbines, which can be potentially used as compressors by controlling the rotor blade pitch, is investigated in [103,104]. Wave power capture can be effectively increased using a variable-pitch turbine, although the compression energy can be significant [103], especially for relatively high incident waves. Finally, an alternative solution for providing reactive power in OWCs is considered [105], where a lightweight piston is used to apply force to the water column and control the hydrodynamic response of an OWC chamber.

5.2.2. Latching

As a simpler (passive, i.e., with no need for bidirectional energy flow) alternative to reactive control, Budal and Falnes proposed a (suboptimal) control method, known as latching [107], which does not require reactive power. In latching, the WEC is hold at a fixed position during a part of the wave cycle, and then released, so that the WEC velocity is in phase with the excitation force. Generally, latching is a suboptimal control approach, as it only focuses on satisfying the phase matching, and not the amplitude matching, conditions of Eq. (39).

Latching for OWCs, first studied in the 1980's [108,109] for fixed OWCs, is implemented by closing/opening a valve (or latching valve) in series with the turbine. OWC latching aims to satisfy the phase matching condition between the velocity and the excitation force. Closing the latching valve significantly reduces OWC motion, but does not completely eliminate water column displacement, due to the spring-like air compressibility effect. A fundamental difference between OWCs and other WEC types is that air compressibility removes the constraint of the latching instant having to coincide with an instance of zero relative velocity. Numerical simulation shows that OWC latching can significantly improve wave energy absorption, when the incident wave frequency is less than the OWC resonant frequency.

The design and operation of a latching valve, which is essentially a HSSV, for axial-flow turbines is a major challenge, due to the relatively large turbine duct diameter [110]. Salter [110] proposed and designed a complex HSSV for the Wells turbine of the Pico power plant, but the valve was never installed. Only the invention of the biradial turbine, which can be equipped with a relatively simple and effective HSSV, opened the possibility for OWC latching, Fig. 8.

A critical issue in OWC latching is the high sensitivity of latching control to a delay between the latching control decision and the actual valve opening/closure [111]. As shown in [106], latching in irregular waves generally requires prior knowledge of the excitation force, from 10s up to 24s into the future, to be effective. Wave forecasting over a sliding time window using, for example, auto-regressive (AR) models or recurrent neural network (RNN) algorithms, can improve latching effectiveness in WECs [27]. Up-wave and auto-regressive wave forecasting methods for an OWC are studied in [112], while a review can be found in [113].

Some OWC latching control strategies, for a spar-buoy equipped with a biradial turbine, are proposed in [114,115]. In [114], a metaheuristic differential evolution (MDE) method is used to optimise the latching/unlatching time instants for numerical simulations in regular waves. Ultimately, latching in regular waves is considerably more straightforward than in irregular waves, since, in regular waves, latching control is simply identically iterated/repeated at each wave cycle, where the latching time can be determined off-line. Latching control becomes much more complicated in irregular waves, as shown (for example) in [115], where two different latching strategies are proposed. Despite providing better performance in terms of absorbed wave power, the first latching strategy in [115] requires future knowledge of the excitation force, while the second latching strategy is based on easily measurable quantities, such as pressure and rotational speed. It should be noted that the first strategy in [115] does not consider possible errors introduced by an inaccurate excitation force prediction, which may have a significant impact on control performance.

Latching control studies for an OWC spar-buoy are also carried out in [106], where a MPC-based latching control approach is numerically tested without considering possible constraints. The control problem (i.e., find the optimal HSSV position to maximise the turbine energy production) is repeatedly solved over a receding horizon, where the excitation force is assumed to be known. Improvements in wave power absorption are only found for receding horizon time windows (sufficiently) larger than the typical energy period at the deployment site. In [116], the unconstrained MPC-based latching control proposed in [106] is extended to take into account some constraints particularly to limit the turbine and generator powers. Ultimately, any OWC control strategy that relies on future information (e.g. wave excitation force) needs to consider inevitable prediction errors and, ideally, mitigate them.

5.2.3. Declutching (or unlatching)

Declutching control disconnects the PTO mechanism from the WEC floater, allowing free movement of the device during part of the wave cycle to accelerate the active PTO component. The PTO mechanism is then engaged at the prescribed/desired velocity [117]. Declutching is the counterpart of latching and mimic resonant conditions when the incident wave frequency is higher than the WEC resonant frequency (i.e. the WEC is speeded up).

The idea behind OWC declutching is to open a bypass valve with small losses to decouple the water column and the PTO mechanism and to close the valve at a later stage of the wave cycle. However, declutching results in a loss of energy from reflected waves due to an impedance mismatch [118]. To the best of the authors' knowledge, declutching has not yet been considered for OWCs. The lack of focus on declutching may be due to the fact that OWC declutching may lead to large water column excursions, which must be limited to prevent green water from reaching the turbine blades (causing damage).

5.3. Power dissipation control

Pressure levels in an OWC chamber can be high, so the maximum instantaneous pneumatic power can be relatively large. In highly energetic sea states, the instantaneous pneumatic power can be more than ten times larger than the generator rated power. Furthermore, under extreme sea state conditions, the turbine/generator set rotational speed could exceed the prescribed safety limits. To prevent this, power dissipation control should be used to dissipate excessive power; otherwise, the OWC device must be shut down to avoid major failure.

There are typically two options to limit available pneumatic power on OWCs. A bypass valve, installed in parallel with the turbine, can be partially opened, or a valve installed in series with the turbine can be partially closed.

5.3.1. Methods based on bypass valves

A bypass valve can be partially, or fully, opened to limit the available pneumatic power in the air chamber. In [30], a possible control law for a bypass valve is proposed to limit the available pneumatic power and, consequently, the rotational speed of the 400 kW Wells turbine installed at the Pico power plant. When the chamber pressure exceeds a prescribed maximum value, $p_c^{\max}$, the area of the bypass valve is changed/controlled as follow

$$\Delta A_v = \alpha \frac{V_0 \sqrt{\rho_{at}}}{p_{at}} \frac{p_c - p_c^{\max}}{\Delta t \sqrt{p_c}}, \tag{40}$$

to keep $p_c = p_c^{\max}$. In Eq. (40), $\alpha > 0$ is a user-defined constant parameter and Δt is the time step used for the numerical simulations. If $p_c \leqslant p_c^{\max}$, the bypass valve is kept closed. Numerical simulations show that, if the relief valve has a suitable dimension, pneumatic power can be effectively dissipated using the control law in Eq. (40), although the achieved control performance depends on the value of α and the time-response of the bypass valve. To counteract possible issues due to the finite time-response, wave prediction can be considered [112].

5.3.2. Methods based on throttle valves

Throttle valves are installed in series with the turbine to induce large pressure losses and, consequently, reduce the available pneumatic power to the turbine [79,83,82]. Typically, butterfly and slide gate valves are used for this purpose. A side effect of throttle valves is the non-axisymmetric flow downstream of these types of valves, typically reducing the turbine performance for one of the flow directions. On the other hand, the built-in valve of the biradial turbine introduces only a local disturbance, which has a negligible effect on the airflow at the turbine rotor level.

5.3.3. Peak-shaving

The small and fast valve in series with the biradial turbine can be used not only (as a HSSV) for latching control, but also for peak-shaving control. Peak-shaving control sets the position of the valve of the biradial turbine to dissipate and limit the available pneumatic power based on the instantaneous rotational speed [28] Peak-shaving control allows OWCs to operate under highly energetic sea states, while avoiding PTO over-speeding and generator overloading and, consequently, increasing the capacity factor and improving the power quality of the electrical energy supplied to the grid. The peak-shaving control algorithm (Fig. 14) was validated in sea trials at the Mutriku wave power plant during the H2020 OPERA project [28].

In contrast to power dissipation methods based on throttle valves (Section 5.3.2), peak-shaving can control almost instantaneously the maximum pneumatic power delivered to the turbine.

5.4. Grid-side control

Although the main focus of this paper is on device-side control

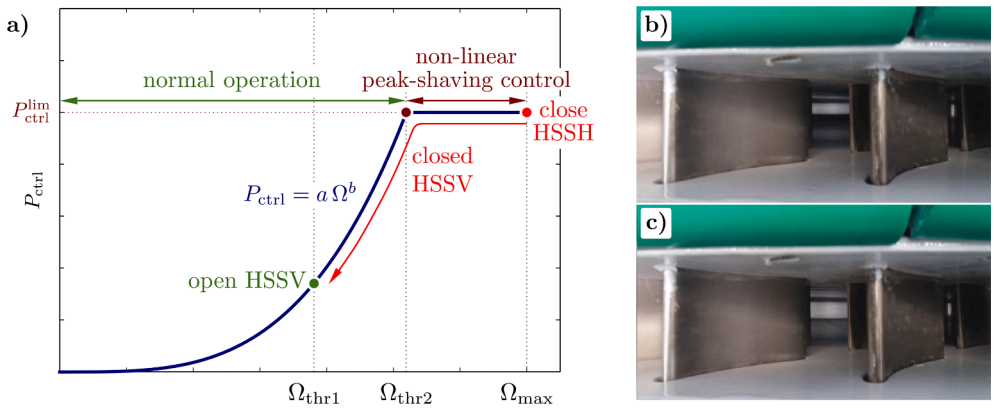

Fig. 14. a) Peak-shaving control algorithm. The HSSV of the biradial turbine installed at the Mutriku wave power plant b) half-open and c) fully closed.

strategies for OWCs, the main studies on OWC grid-side control are briefly discussed. Grid-side control, and energy storage methods, cope with grid requirements, which mainly concern power quality aspects, fault-ride-through (FRT) capabilities, and, more generally, the overall stability of the power grid. An overview of grid integration aspects of wave energy can be found in [131].

In [132,133], a control strategy to improve the FRT capability of a DFIG coupled with a Wells turbine is numerically tested, while robust control under fault conditions is studied in [134]. Some MPC strategies, to improve power quality for grid-side converters, are also considered in [95,135,136,96].

Studies on electrical energy storage systems for power smoothing, using supercapacitors [137,138], ultracapacitors [89], and Li-ion batteries [95], can also be found. In contrast to other WEC types, power smoothing on OWCs may be less important, due to the capability of smoothing power peaks on the device-side through, for instance, control valves.

6. Summary of control strategies

Table 1 summarises the broad classification of OWC control strategies proposed in Section 5. The continuous horizontal lines separate different control objectives, the dashed lines divide the specific control approaches, and the dotted lines separate different control philosophies (e.g., PID and SMC).

From Table 1, it is clear that OWC control strategies mainly focus on turbine control, which is typically implemented using a torque and/or a throttle valve controller, while only a limited number of studies concern hydrodynamic control (mainly latching). The focus on turbine control can be motivated by different convictions. First, if the turbine operates far from its maximum efficiency point, it is impossible to achieve satisfactory power production. Furthermore, turbine control (as a setpoint-following problem) is a relatively straightforward control problem, which can be tackled using a wide variety of different controllers.

In addition to the significant attention on turbine control, Table 1 also reflects the lack of focus on hydrodynamic control, for the following reasons. Firstly, OWC hydrodynamic control is somewhat difficult to implement, especially due to the absence of suitable actuators for providing direct reactive (pneumatic/aerodynamic) power. Moreover, although latching control does not need reactive power, the practical implementation of latching for OWCs became possible only following the emergence of the biradial turbine. Finally, in the case of a Wells turbine, simultaneously optimising turbine efficiency and hydrodynamic performance is difficult due to the effect of the hydrodynamic/aerodynamic interaction (which is typically neglected to simplify the Wells turbine control problem to a setpoint following problem). Ultimately, OWC hydrodynamic control is still a relatively unexplored area of OWC control.

Finally, power dissipation control typically relies on relatively simple and effective methods based on control valves. Peak-shaving control appears to be the best solution to limit the pneumatic power available to the turbine, while greatly improving the system capacity factor. A possible alternative to methods based on control valves is to consider rotor blade pitch control, widespread in wind energy [139]. Pitch control reduces the turbine aerodynamic shaft power by decreasing the angle of attack of the rotor blades. However, since it requires a relatively complex blade-pitching mechanism, likely resulting in higher capital and operational costs, pitch control has not yet been applied on OWCs.

7. Perspectives and future directions

In OWC control history, since the air turbine is the most sensitive component of the PTO system to control, there has been an understandable focus on turbine efficiency maximisation. Indeed, appropriate control of the turbine rotational speed is essential to produce a satisfactory amount of electric energy, especially in Wells turbines, which are characterised by a relatively narrow and peaky efficiency curve, if compared to impulse-like self-rectifying turbines.

To date, although the main control objective has been turbine efficiency maximisation, the OWC research community has also focussed on other aspects of OWC control, such as power quality aspects, and peak-shaving control for increasing the capacity factor of the OWC system. From the authors' perspective, too much attention is still dedicated to issues of secondary importance, such as finding new types of controllers for the (turbine rotational speed) setpoint following problem, which is a relatively standard problem in control systems, while there is an apparent lack of interest in improving the W2W system performance (which is where the possibility for substantial innovation truly lies).

In the future, to improve overall OWC system performance, it will be essential to consider a more complete control objective, since turbine efficiency maximisation alone does not guarantee W2W efficiency maximisation. In light of this, a composite rotational speed setpoint, which considers the characteristics of the whole W2W OWC system, should be sought.

In the current section, perspectives and possible future directions in terms of control objectives (Section 7.1), other control possibilities (Section 7.2), and control co-design (Section 7.3) are discussed.

7.1. Control objectives

To improve the economic viability of OWC WECs, it is essential to minimise LCoE, since maximising power production only does not necessarily guarantee economic advantage. Despite the fact that the ultimate control objective, i.e., LCoE minimisation, is difficult, especially due to the problem of OpEx estimation, it is important to make

Table 1
Control strategies for oscillating water column wave energy converters. Part 1 of 2: Turbine control. Notes: Turbine types are denoted as follows: Wells (W), axial-flow impulse (I), biradial (B), unidirectional (U), and, if both Wells and biradial turbines are considered, the turbine type is denoted as B/W. Test type indicates if the control strategy is tested in numerical simulation (Num) and/or in experimental tests (Exp). Manipulated inputs are reported following the notation used in Fig. 3. For combined control strategies which use multiple control inputs, all control inputs are reported and separated by a slash (e.g., $T_{ctrl}/u_{throttle}$).

Control objective	Control approach	Turbine type	Ref.	Test type	Year	Controller	Manipulated input
Turbine control							
	Setpoint determination	B	[119]	Num/Exp	2016	ACL	T_{ctrl}/u_{bypass}
		B/W	[32]	Num/Exp	2019	ACL	T_{ctrl}/u_{hssv} T_{ctrl}/u_{hssv}
		U	[69,70]	Exp	2020–21	ACL	T_{ctrl}
		–	[120]	Num	2022	ACL	T_{ctrl}/u_{hssv}
	Setpoint following	W	[78]	Num	2011	PI	T_{ctrl}
		W	[79,80]	Num/Exp	2011–13	ZN-PID PI/PID	$u_{throttle}$ $T_{ctrl}/u_{throttle}$
		W	[77,89]	Num/Exp	2013–15	ZPC-PI	T_{ctrl}
		W	[74]	Num	2016	P	T_{ctrl}
		W	[82]	Num	2017	PSO-PID	$u_{throttle}$
		W	[83]	Num	2019	FPSOM-PID HS-PID	$u_{throttle}$ $u_{throttle}$
		I	[81]	Num	2019	FGS-PID GGW-PID	$u_{throttle}$ T_{ctrl}
		W	[84,85]	Num	2011–20	ANN-PI	T_{ctrl}
		W	[86]	Num	2020	SGHS-PID	$u_{throttle}$
		W	[87]	Num	2020	PSO-PID	$u_{throttle}$
		W	[88]	Num	2020	ANN-PI	$u_{throttle}$
		W	[121]	Num	2012	SMC	T_{ctrl}
		W	[122]	Num	2018	SMC	T_{ctrl}
		W	[92]	Num	2018	SMC	T_{ctrl}
		W	[123]	Num	2018	SMC	T_{ctrl}
		B	[91]	Num	2019	SMC	T_{ctrl}/u_{hssv}
		I	[124]	Num	2019	GGW-SOSMC	T_{ctrl}
		W	[93]	Num	2020	FGS-SMC	T_{ctrl}
		W	[73]	Num	2020	SOSMC	T_{ctrl}
		B	[125]	Num	2020	SOSMC	T_{ctrl}
		B	[75]	Num	2021	SOSMC	T_{ctrl}/u_{hssv}
		U	[95]	Num	2017	MPC	T_{ctrl}
		W	[96]	Num/Exp	2021	MPC	T_{ctrl}
		W	[123]	Num	2018	BS	T_{ctrl}
		W	[98]	Num	2020	BS	T_{ctrl}

(continued on next page)

Table 1 (*continued*)

Control	Control	Turbine	Ref.	Test	Year	Controller	Manipulated
		W	[99]	Num	2021	FLC	T_{ctrl}
		I	[126,127]	Num	2015 –16	–	T_{ctrl}
		W	[20]	Num	1999	–	$u_{bypass}/u_{throttle}$

Table 1: Part 2 of 2: Hydrodynamic control and power dissipation.

Control objective	Control approach	Turbine type	Ref.	Test type	Year	Controller	Manipulated input
Hydrodynamic control							
	Reactive						
		–	[105,128]	Exp	1991	–	–
		W	[104,103]	Num	2003	–	u_{pitch}
	Latching						
		B	[114,115]	Num	2013–14	–	u_{hssv}
		B	[106,116]	Num/Exp	2016	MPC	u_{hssv}
		W	[129]	Num	2016	–	u_{hssv}
		B	[130]	Num	2017	–	u_{hssv}
Power dissipation							
	Methods based on valves						
		W	[76]	Num	1999	–	u_{bypass}
		W	[30]	Num	2003	–	u_{bypass}
		B	[28]	Num	2019	–	u_{hssv}
		B	[75]	Num	2021	–	u_{hssv}

progress towards LCoE minimisation. Specifically, from a control design perspective, the focus is on what elements of CapEx and OpEx (see Eq. (1)) are sensitive to control system specification (mostly CapEx) or control system operation (mostly OpEx).

Regarding CapEx, the main design decisions relate to the PTO power specification and the OWC device structure. If a high rated power is demanded, the system can cope with the widest possible set of sea states, but may be significantly over-specified in moderate (and probably most frequent) sea states and lead to rather low time-averaged electrical efficiency. In this scenario, the capacity factor is likely to be low and a relatively high LCoE may result. However, the need to dissipate power, for example through peak shaving (Section 5.3.3) may be virtually eliminated, simplifying the operation of the control system and requirement for throttle valves.

A relatively minor consideration, regarding CapEx, is the requirement for specific actuators, or measurements, by particular control philosophies. However, in general, actuators and sensors may be considered to be a relatively tiny fraction of CapEx, compared to the considerable cost of the OWC device structure (or OWC 'hull'), along with electrical interconnection and mooring costs (for floating devices).

Of the three constituent terms in Eq. (1), OpEx is the most difficult to quantify. However, from a control design perspective, the important aspect is to assess components of OpEx which are sensitive to control actions. To date, little progress has been made in relating control action to WEC OpEx, though some studies are appearing [15]. However, to the best of the authors' knowledge, no studies linking control actions to OpEx for OWCs have yet been published.

An alternative economic objective could be considered as capacity factor. However, this is strongly related to LCoE and is more a function of the power capacity rating of the system, than energy maximising control. Nevertheless, capacity factor, as an objective, could have a role in control co-design, or supervisory control.

7.2. Other control possibilities

Generally, new control possibilities for OWC WECs will fall into either (i) optimisation problems, which can be convex or non-convex, or (ii) tracking problems. Regarding non-convex optimisation problems (which presents multiple local minima), non-convex optimisation algorithms, with a relatively high computational cost, could be used only if the optimisation problem is solved off-line. However, in real-time control, non-convex optimisation algorithms cannot generally be used due to excessive computational burden and, therefore, convexification techniques have to be adopted to turn the non-convex optimisation problem into a convex one. A convex optimisation problem can then be solved with relatively fast optimisation algorithms, such as line search methods. Optimisation problems can be presented in terms of W2W control, or as part of a control co-design problem, where aspects of the system structure, capacity, or ratings are optimised, in tandem with the control system. As already stated, tracking problems can be divided into two sub-problems, a setpoint determination problem, and a setpoint following problem. In addition to PID and SMC, the setpoint following problem could be solved using a multitude of other controllers, well documented in the traditional regulator/servomechanism control system literature [140]. However, since good tracking performance in OWCs can be achieved with currently available controllers (e.g., SMC),

finding new types of controllers for the setpoint following problem is of marginal importance and should not be prioritised among other possible future studies. In OWCs, the most interesting possibilities for innovating the tracking problem lie in the setpoint determination problem. A difficult problem is to determine the optimum rotational speed setpoint for Wells turbines, while considering the hydrodynamic/aerodynamic interaction. For a Wells turbine, is the combined hydrodynamic/aerodynamic control strategy worth the effort (modelling and control design) or any additional cost in sensors/actuators? Or is turbine efficiency maximisation the most practical way to maximise energy production?.

Concerning model-based control approaches, the use of *control-oriented* models (e.g., data-based models) and/or more accurate models (e.g., for the hydrodynamic part, the uniform pressure model is more realistic than the piston model) may potentially improve control performance, provided that model accuracy and complexity are balanced. We must refrain from using unnecessarily complex models, since the cost of the computation may become too large for real-time control application. Furthermore, the impact of model uncertainty (e.g., uncertainty in the hydrodynamic model) on control performance should be considered. Recently, some robust control studies for other forms of WEC have begun to appear [141–143] though no studies focusing on the robust control of OWCs have yet emerged.

Finally, to address the lack of focus on hydrodynamic control, alternative strategies to implement OWC hydrodynamic control could be considered.

7.3. Control co-design

Although some studies on OWC WEC design (e.g., a step in front of the OWC device [144], and shape of the chamber front wall to reduce viscous losses [145]) can be found, they do not usually consider interaction with control aspects.

In future studies, control co-design techniques [146] should be adopted to guarantee the best *control-informed* OWC WEC design. One advantage of examining the overall system design within a control framework is that the contribution to the overall system dynamics by both the OWC structure and the controller can be seen side-by-side, and the most efficacious way of optimising the system performance identified. Indeed, the optimum OWC WEC design for the uncontrolled device case may significantly differ from the optimum design found for the controlled device case, and, moreover, different optimal geometries (OWC 'hull' and turbine geometry) could be obtained for different control strategies [146]. It should be noted that control co-design is particularly important for the Wells turbine case, since the turbine rotational speed affects the hydrodynamic performance.

An important issue related to co-design is the selection of suitable control actuators. Control actions, provided by real control actuators, and ultimate control performance, are intrinsically limited by the physical range of the actuators, and actuator availability, respectively. Actuators with a larger operational range may lead to higher produced power, but are generally more expensive, and, therefore, a trade-off between CapEx and reward (e.g., produced power) should be made when selecting the control actuators. Since control possibilities change if an actuator is used singly, or in combination with another actuator, the selection of suitable control actuators also depends on which types of actuators are available. In relation to this, it should be noted that the control problem, as well as the control possibilities (e.g., the potentially available actuators), depend on the characteristics of the type of air turbine mounted on the OWC device.

8. Conclusions

This paper aims to provide a comprehensive analysis of the control problem for OWCs, together with a review of the existing control strategies. Since enclosing all the control strategies found in the literature in a rigid classification would be difficult, a broad objective-focused classification approach has been taken.

Ultimately, the OWC control problem can be tackled at different stages of the energy conversion chain. However, the vast majority of control strategies found in the literature focus on turbine rotational speed control. Indeed, if the turbine operates far from its maximum efficiency point, the overall system efficiency is highly penalised and, consequently, poor electrical power production is achieved.

Since the sea state can significantly vary during a WEC's lifetime, to maximise power production, real-time control techniques should be adopted and, to this end, it is essential to keep the OWC model relatively simple, hence computationally fast. Furthermore, to develop comprehensive control strategies which can maximise the overall efficiency of the device, the complete (and computationally simple) W2W OWC system, as well as all the possible control effectors, should be considered. Finally, to guarantee optimal control-informed WEC design, control-related aspects should be considered since from the initial stages of the WEC design phase and, to this end, a co-design approach should be adopted.

Despite robust control strategies can improve power production [147], most studies on OWC control ignore the impact of model uncertainty on the control actions. However, the importance of assessing the influence of uncertainty on the performance of the control strategies should not be overlooked. In wave energy, model uncertainties may be due to: assumptions (e.g., LPT) and simplifications of the mathematical model, unmodelled dynamics (e.g., neglected nonlinear effects), inaccuracy in model parameters, inaccurate measurements of the physical variables and, when predictions are needed, errors in wave forecasting/estimation.

In summary, given the relative youth of OWC design and control, and the relatively large range of currently unexplored control and optimisation possibilities, there is considerable scope to reduce OWC LCoE to make them economically competitive with other renewable, and traditional, energy conversion forms.

Declaration of Competing Interest

The authors declare that they have no known competing financial interests or personal relationships that could have appeared to influence the work reported in this paper.

Acknowledgements

Thanks are due to CarrieAnne Barry of the Centre for Ocean Energy Research (COER) at Maynooth University for providing language help. This paper is based upon work supported by: i) Marine and Renewable Energy Ireland (MaREI), the Science Foundation Ireland (SFI) Research Centre for Energy, Climate and Marine, under Grant No. 12/RC/2302_P2; and ii) Portuguese Foundation for Science and Technology (FCT), through IDMEC, under LAETA project UID/EMS/50022/2020.

Appendix A. Comparing air and water turbines for OWCs

The use of self-rectifying water turbines for OWCs has three major drawbacks. The first problem is the possibility of the occurrence of cavitation. Cavitation is a major issue, especially for Wells turbines due to the large suction peaks achieved at the leading edge of the turbine rotor blades for large pressure coefficients. The second and third problems for water turbines are, respectively, the very low rotational speed and the large turbine rotor

diameter. The problems associated with rotational speed and rotor diameter are easily shown assuming geometric similar turbines (i.e, equal dimensionless geometry) and comparing air and water turbines. The turbine flow rate (neglecting air compressibility effects, which are small in this comparative analysis) and the turbine power are equal for water and air, i.e., $Q_{\text{turb}}^{\text{water}} = Q_{\text{turb}}^{\text{air}}$ and $P_{\text{turb}}^{\text{water}} = P_{\text{turb}}^{\text{air}}$. As such, the turbine operating point is the same for both types of turbines and, consequently, $\Phi_{\text{air}} = \Phi_{\text{water}}$ and $\Pi_{\text{air}} = \Pi_{\text{water}}$. Solving for the diameter and rotational speed, we get the following ratios

$$\frac{d^{\text{water}}}{d^{\text{air}}} = \left(\frac{\rho_{\text{water}}}{\rho_{\text{air}}}\right)^{1/4} = 5.35, \tag{A.1}$$

and

$$\frac{\Omega_{\text{water}}}{\Omega_{\text{air}}} = \left(\frac{\rho_{\text{air}}}{\rho_{\text{water}}}\right)^{3/4} = \frac{1}{153.2}. \tag{A.2}$$

Eq. (A.2) implies that for obtaining the same turbine power, the torque ratio is $T_{\text{water}}/T_{\text{air}} = 153.2$.

Appendix B. Conversion of Maeda's et al. dimensionless numbers

Maeda et al. [41] proposed the following flow, "input" and torque coefficients

$$C_A(\phi) = \frac{p_c Q}{\frac{1}{2}\rho\left(v_x^2 + U_r^2\right) b\ell Z v_x}, \tag{A.3}$$

$$C_T(\phi) = \frac{T}{\frac{1}{2}\rho\left(v_x^2 + U_r^2\right) b\ell Z R_r}, \tag{A.4}$$

obtained experimentally as a function of

$$\phi = \frac{v_x}{U_r}, \tag{A.5}$$

where b is the blade height, ℓ the blade chord, Z the number of rotor blades, R_r the mean radius and v_x is the mean axial velocity. The circumferential velocity at mean radius is defined by

$$U_r = \Omega R_r. \tag{A.6}$$

The flow rate, Q, is related to the mean axial velocity, v_x, through $Q = v_x A$, where A is the area of the turbine duct.

To solve ODE (5) we need to compute $w_{\text{turb}} = \rho_{\text{in}} Q$ as a function of p_c. This computation is simple if the turbine is modelled with Eq. (19), but that is not the case of Eq. (A.5). Given p_c, the axial velocity is computed from the pressure expressing (A.3) as

$$C_A(\phi)\left(v_x^2 + U_r^2\right) = \frac{p_c A}{\frac{1}{2}\rho b\ell Z}. \tag{A.7}$$

This equation shows that it is impossible to find an explicit relationship to determine v_x as a function of p_c, since ϕ also depends on v_x.

The conversion of Maeda's dimensionless numbers to the set numbers defined in Eqs. (23)–(20) is as follows. Writing the flow rate Q as function of (19) and (A.5), and using (A.6) we found that $\Phi d^3\Omega = \phi A \Omega R_r$, yielding

$$\Phi = A R_r \phi / d^3. \tag{A.8}$$

Expressing the pressure difference p_c as function of (23) and (A.3), results

$$\Psi \rho \Omega^2 d^2 = \frac{1}{2}\rho\left(v_x^2 + U_r^2\right)\frac{b\ell Z}{A} C_A. \tag{A.9}$$

Using the definition of the flow rate coefficient (A.5) and (A.6), we get

$$\Psi = \frac{1}{2}\left(\phi^2 + 1\right)\frac{b\ell Z R_r^2}{A d^2} C_A. \tag{A.10}$$

Analogously, we can write the Π as function of ϕ using (20) and (A.4), giving

$$\Pi = \frac{1}{2}\left(\phi^2 + 1\right) C_T \frac{b\ell Z R_r^3}{d^5}. \tag{A.11}$$

Functions (A.8) and (A.11) are expressed as a function of (A.10), and this conversion is applied for each set of b, ℓ, z and R_r.

References

[1] Y. Masuda, Wave-activated generator, Int. Coll. on the Expositions of the Oceans (Trans.), Bordeaux, France.
[2] Ross D. Power from the Waves. USA: Oxford University Press; 1995.
[3] M. Boland, T. Kelly, R. Carolan, B. Walsh, T. Dooley, Scale model testing of the WASP – a novel wave measuting buoy, in: Proceedings of the 13th European Wave and Tidal Energy Conference, Naples, Italy, 2019, pp. 1–9. URL: http://www.bolandengineering.ie/resources/Scale%20model%20testing%20of%20the%20WASP.pdf.
[4] Y. Torre-Enciso, I. Ortubia, L.L. De Aguileta, J. Marqués, Mutriku wave power plant: From the thinking out to the reality, in: Proceedings of the 8th European Wave and Tidal Energy Conference, Uppsala, Sweden, 2009, pp. 319–329. URL: https://tethys.pnnl.gov/sites/default/files/publications/Torre-Enciso_et_al_2009.pdf.
[5] F. Arena, V. Fiamma, V. Laface, G. Malara, A. Romolo, A. Viviano, G. Sannino, A. Carillo, Installing U-OWC devices along italian coasts, in: Proceedings of the 32nd International Conference on Ocean, Offshore and Arctic Engineering, Nantes, France, 2013. doi:10.1016/j.renene.2016.07.080.
[6] A. Fleming, G. MacFarlane, S. Hunter, T. Denniss, Power performance prediction for a vented oscillating water column wave energy converter with a unidirectional air turbine power take-off, in: Proceedings of the 12th European Wave and Tidal Energy Conference, Cork, Ireland, 2017. URL: https://eprints.utas.edu.au/25089/.
[7] Falcão AFO, Henriques JCC, Cândido JJ. Dynamics and optimization of the OWC spar buoy wave energy converter. Renewable Energy 2012;48:369–81. https://doi.org/10.1016/j.renene.2012.05.009.
[8] Masuda Y, McCormick ME. Experiences in pneumatic wave energy conversion in Japan. In: Costal Engineering. ASCE, Taipei, Taiwan; 1986. p. 1–33. URL:https://cedb.asce.org/CEDBsearch/record.jsp?dockey=0054744.
[9] Falcão AFO, Henriques JCC. Oscillating-water-column wave energy converters and air turbines: A review. Renewable Energy 2016;85:1391–424. https://doi.org/10.1016/j.renene.2015.07.086.
[10] Falcão AFO, Gato LMC. Air turbines. In: Sayigh A, editor. Comprehensive Renewable Energy, vol. 8. Oxford: Ocean E, Elsevier; 2012. p. 111–49. https://doi.org/10.1016/B978-0-08-087872-0.00805-2.
[11] Falcão AFO, Henriques JCC, Gato LMC. Self-rectifying air turbines for wave energy conversion: A comparative analysis. Renew Sustain Energy Rev 2018;91:1231–41. https://doi.org/10.1016/j.rser.2018.04.019.
[12] Astariz S, Iglesias G. The economics of wave energy: A review. Renew Sustain Energy Rev 2015;45:397–408. https://doi.org/10.1016/j.rser.2015.01.061.
[13] Chang G, Jones CA, Roberts JD, Neary VS. A comprehensive evaluation of factors affecting the levelized cost of wave energy conversion projects. Renewable Energy 2018;127:344–54. https://doi.org/10.1016/j.renene.2018.04.071.
[14] Bull D, Ochs ME. Technological cost-reduction pathways for oscillating water column wave energy converters in the marine hydrokinetic environment. Albuquerque, New Mexico and Livermore, California: Sandia National Laboratories; 2013. URL:https://core.ac.uk/reader/208687161 Tech. rep.,.
[15] Nielsen KM, Pedersen TS, Andersen P, Ambühl S. Optimizing control of wave energy converter with losses and fatigue in power take off. IFAC-PapersOnLine 2017;50(1):14680–5. https://doi.org/10.1016/j.ifacol.2017.08.2497.
[16] Bacelli G, Coe RG. Comments on control of wave energy converters. IEEE Trans Control Syst Technol 2020;29(1):478–81. https://doi.org/10.1109/TCST.2020.2965916.
[17] Guo B, Ringwood JV. Geometric optimisation of wave energy conversion devices: A survey. Appl Energy 2021;297:117100.
[18] O'Sullivan DL, Lewis AW. Generator selection and comparative performance in offshore oscillating water column ocean wave energy converters. IEEE Trans Energy Convers 2011;26(2):603–14. https://doi.org/10.1109/TEC.2010.2093527.
[19] Thomsen JB, Ferri F, Kofoed JP, Black K. Cost optimization of mooring solutions for large floating wave energy converters. Energies 2018;11(1):159. https://doi.org/10.3390/en11010159.
[20] Falcão AFO, Justino PAP. OWC wave energy devices with air flow control. Ocean Eng 1999;26(12):1275–95. https://doi.org/10.1016/S0029-8018(98)00075-4.
[21] O'Sullivan ACM, Lightbody G. Co-design of a wave energy converter using constrained predictive control. Renewable Energy 2017;102:142–56. https://doi.org/10.1016/j.renene.2016.10.034.
[22] M. Durand, A. Babarit, B. Pettinotti, O. Quillard, J. Toularastel, A. Clément, Experimental validation of the performances of the searev wave energy converter with real time latching control, EWTEC, Porto.
[23] Said HA, García-Violini D, Ringwood JV. Wave-to-grid (W2G) control of a wave energy converter. Energy Conversion and Management: X 2022;14:100190. https://doi.org/10.1016/j.ecmx.2022.100190.
[24] Korde UA, Ringwood JV. Hydrodynamic control of wave energy devices. Cambridge University Press 2016. https://doi.org/10.1017/CBO9781139942072.
[25] Xie J, Zuo L. Dynamics and control of ocean wave energy converters. Int J Dyn Control 2013;1(3):262–76. https://doi.org/10.1007/s40435-013-0025-x.
[26] Coe RG, Bacelli G, Wilson DG, Abdelkhalik O, Korde UA, Robinett III RD. A comparison of control strategies for wave energy converters. Int J Mar Energy 2017;20:45–63. https://doi.org/10.1016/j.ijome.2017.11.001.
[27] A. Rahoor, Comparison of control strategies for wave energy converters, Tech. rep., Master Programme in Renewable Electricity Production, Upsalla Universitet (2020). URL: https://www.diva-portal.org/smash/record.jsf?pid=diva2%3A1478215&dswid=7243.
[28] J.C.C. Henriques, A.A.D. Carrelhas, L.M.C. Gato, A.F.O. Falcão, J.C.C. Portillo, J. Varandas, Peak-shaving control – A new control paradigm for OWC wave energy converters, in: Proceedings of the 12th European Wave and Tidal Energy Conference, Cork, Ireland, 2017.
[29] Monk K, Winands V, Lopes M. Chamber pressure skewness corrections using a passive relief valve system at the pico oscillating water column wave energy plant. Renewable Energy 2018;128:230–40. https://doi.org/10.1016/j.renene.2018.04.037.
[30] A.F. de O. Falcão, L.C. Vieira, P.A.P. Justino, J.M.C.S. André, By-Pass Air-Valve Control of an OWC Wave Power Plant, J Offshore Mech Arctic Eng 125 (3) (2003) 205–210. doi:10.1115/1.1576815.
[31] Falcão AFO, Henriques JCC. Effect of non-ideal power take-off efficiency on performance of single-and two-body reactively controlled wave energy converters. J Ocean Eng Mar Energy 2015;1(3):273–86. https://doi.org/10.1007/s40722-015-0023-5.
[32] Henriques JCC, Portillo JCC, Sheng W, Gato LMC, Falcão AFO. Dynamics and control of air turbines in oscillating-water-column wave energy converters: Analyses and case study. Renew Sustain Energy Rev 2019;112:571–89. https://doi.org/10.1016/j.rser.2019.05.010.
[33] G.B. Airy, Tides and waves, Encyclopaedia Metropolitana, Mixed Sciences 3.
[34] Evans D. The oscillating water column wave-energy device. IMA J Appl Math 1978;22(4):423–33. https://doi.org/10.1093/imamat/22.4.423.
[35] T. Kelly, T. Dooley, J.V. Ringwood, Experimental determination of the hydrodynamic parameters of an OWC, in: Proceedings of the 12th European Wave and Tidal Energy Conference, Cork, Ireland, 2017, pp. 1–10. URL: https://mural.maynoothuniversity.ie/12459/.
[36] Kelly T. Experimental and numerical modelling of a multiple oscillating water column structure. National University of Ireland Maynooth; 2018. Ph.D. thesis, URL:https://www.proquest.com/docview/2187528122?pq-origsite=gscholar&fromopenview=true.
[37] Evans DV. Wave-power absorption by systems of oscillating surface pressure distributions. J Fluid Mech 1982;114:481–99. https://doi.org/10.1017/S0022112082000263.
[38] Falnes J, Kurniawan A. Ocean waves and oscillating systems: linear interactions including wave-energy extraction, vol. 8. Cambridge University Press; 2020.
[39] Falcão AFO, Henriques JCC. The spring-like air compressibility effect in OWC wave energy converters: Hydro-, thermo-and aerodynamic analyses. In: International Conference on Offshore Mechanics and Arctic Engineering. Madrid, Spain: American Society of Mechanical Engineers; 2018. https://doi.org/10.1016/j.rser.2019.04.040.
[40] Dixon SL, Hall C. Fluid mechanics and thermodynamics of turbomachinery. Butterworth-Heinemann; 2013.
[41] Maeda H, Santhakumar S, Setoguchi T, Takao M, Kinoue Y, Kaneko K. Performance of an impulse turbine with fixed guide vanes fn2 for wave power conversion. Renewable Energy 1999;17(4):533–47. https://doi.org/10.1016/S0960-1481(98)00771-X.
[42] Abad G, Lopez J, Rodriguez M, Marroyo L, Iwanski G. Doubly fed induction machine: modeling and control for wind energy generation, vol. 85. John Wiley & Sons; 2011.
[43] Vas P. Sensorless vector and direct torque control. Oxford University Press; 1998.
[44] Ljung L. System identification: Theory for the User. Prentice Hall; 1999.
[45] M. Rosati, T. Kelly, G.D. Violini, J.V. Ringwood, Data-based hydrodynamic modelling of a fixed OWC wave energy converter, in: Proceedings of the 14th European Wave and Tidal Energy Conference, Plymouth, UK, 2021, pp. 1–10. URL: https://www.researchgate.net/publication/354544067_Data-based_hydrodynamic_modelling_of_a_fixed_OWC_wave_energy_converter.
[46] Rosati M, Kelly T, Ringwood JV. Nonlinear data-based hydrodynamic modeling of a fixed oscillating water column wave energy device. IEEE Access 2021;9:149756–65. https://doi.org/10.1109/ACCESS.2021.3125600.
[47] Ljung L. Perspectives on system identification. Annu Rev Control 2010;34(1):1–12. https://doi.org/10.1016/j.arcontrol.2009.12.001.
[48] Giorgi S, Davidson J, Ringwood JV. Identification of wave energy device models from numerical wave tank data–part 2: Data-based model determination. IEEE Trans Sustain Energy 2016;7(3):1020–7. https://doi.org/10.1109/TSTE.2016.2515500.
[49] Davidson J, Giorgi S, Ringwood JV. Linear parametric hydrodynamic models for ocean wave energy converters identified from numerical wave tank experiments. Ocean Eng 2015;103:31–9. https://doi.org/10.1016/j.oceaneng.2015.04.056.
[50] Windt C, Faedo N, Penalba M, Dias F, Ringwood JV. Reactive control of wave energy devices–the modelling paradox. Appl Ocean Res 2021;109:102574. https://doi.org/10.1016/j.apor.2021.102574.
[51] Davidson J, Giorgi S, Ringwood JV. Identification of wave energy device models from numerical wave tank data–part 1: Numerical wave tank identification tests. IEEE Trans Sustain Energy 2016;7(3):1012–9. https://doi.org/10.1109/TSTE.2016.2515512.
[52] Wells AA. Fluid driven rotary transducer. British Patent Spec No 1976;1595700.
[53] Henriques JCC, Gato LMC. Use of a residual distribution Euler solver to study the occurrence of transonic flow in Wells turbine rotor blades. Comput Mech 2002;29(3):243–53. https://doi.org/10.1007/s00466-002-0337-8.
[54] M. Takao, K. Itakura, T. Setoguchi, T.H. Kim, K. Kaneko, M. Inoue, Noise characteristics of turbines for wave power conversion, in: Proceedings of the Eleventh International Ocean and Polar Engineering Conference, Stavanger, Norway, 2001. URL: https://onepetro.org/ISOPEIOPEC/proceedings-pdf/ISOPE01/All-ISOPE01/ISOPE-I-01-091/1900904/isope-i-01-091.pdf.
[55] Shehata AS, Xiao Q, Selim MM, Elbatran A, Alexander D. Enhancement of performance of wave turbine during stall using passive flow control: First and

second law analysis. Renewable Energy 2017;113:369–92. https://doi.org/10.1016/j.renene.2017.06.008.
[56] Shehata AS, Xiao Q, Kotb MA, Selim MM, Elbatran A, Alexander D. Effect of passive flow control on the aerodynamic performance, entropy generation and aeroacoustic noise of axial turbines for wave energy extractor. Ocean Eng 2018; 157:262–300. https://doi.org/10.1016/j.oceaneng.2018.03.053.
[57] Maeda H, Setoguchi T, Kaneko K, Kim T, Inoue M, et al. The effect of turbine geometry on the performance of impulse turbine with self-pitch-controlled guide vanes for wave power conversion. In: The Fourth International Offshore and Polar Engineering Conference, International Society of Offshore and Polar Engineers. Osaka, Japan; 1994. URL:https://onepetro.org/ISOPEIOPEC/proceedings-abstract/ISOPE94/All-ISOPE94/ISOPE-I-94-054/25477.
[58] Takao M, Kinoue Y, Setoguchi T, Obayashi T, Kaneko K. Impulse turbine with self-pitch-controlled guide vanes for wave power conversion (effect of guide vane geometry on the performance). Int J Rotating Mach 2000;6(5):355–62. https://doi.org/10.1155/S1023621X00000336.
[59] Dresser-Rand, Hydroair variable radius turbine, URL: http://www.dresser-rand.com/literature/general/2210_HydroAir.pdf (accessed 25 April 2011) (2011).
[60] M.E. McCormick, J.G. Rehak, B.D. Williams, An experimental study of a bidirectional radial turbine for pneumatic wave energy conversion, in: OCEANS 92 Proceedings of the Mastering the Oceans Through Technology, Vol. 2, 1992, pp. 866–870. doi:10.1109/OCEANS.1992.607698.
[61] Saad M, Díaz MG, Pereiras B, González J. Optimized geometry design of a radial impulse turbine for OWC wave energy converters. Appl Ocean Res 2021;111: 102650. https://doi.org/10.1016/j.apor.2021.102650.
[62] Falcão AFO, Gato LMC, Nunes EPAS. A novel radial self-rectifying air turbine for use in wave energy converters. Renewable Energy 2013;50:289–98. https://doi.org/10.1016/j.renene.2012.06.050.
[63] Gato LMC, Maduro AR, Carrelhas AAD, Henriques JCC, Ferreira DN. Performance improvement of the biradial self-rectifying impulse air-turbine for wave energy conversion by multi-row guide vanes: Design and experimental results. Energy 2021;216:119110. https://doi.org/10.1016/j.energy.2020.119110.
[64] J.R.M. Taylor, N.J. Caldwell, Design and construction of the variable-pitch air turbine for the azores wave energy plant, in: Proceedings of the Third European Wave Power Conference, vol. 30, Patras, Greece, 1998.
[65] Gareev A. Analysis of variable pitch air turbines for oscillating water column (OWC) wave energy converters. University of Wollongong; 2011. Ph.D. thesis,.
[66] Gato LMC, Webster M. An experimental investigation into the effect of rotor blade sweep on the performance of the variable-pitch wells turbine. Proc Inst Mech Eng, Part A: J Power Energy 2001;215(5):611–22. https://doi.org/10.1243/0957650011538848.
[67] Curran R, Denniss T, Boake C. Multidisciplinary Design For Performance: Ocean Wave Energy Conversion. USA: Seattle; 2000.
[68] Benreguig P, Vicente M, Dunne A, Murphy J. Modelling approaches of a closed-circuit OWC wave energy converter. J Mar Sci Eng 2019;7(2):23. https://doi.org/10.3390/jmse7020023.
[69] Carrelhas AAD, Gato LMC, Falcão AFO, Henriques JCC. Control law design for the air-turbine-generator set of a fully submerged 1.5 MW mwave prototype. part 2: Experimental validation. Renewable Energy 2021;171:1002–13. https://doi.org/10.1016/j.renene.2021.02.128.
[70] Carrelhas AAD, Gato LMC, Falcão AFO, Henriques JCC. Control law design for the air-turbine-generator set of a fully submerged 1.5 MW mwave prototype. part 1: Numerical modelling. Renewable Energy 2022;181:1402–18. https://doi.org/10.1016/j.renene.2021.09.011.
[71] Gato LMC, Carrelhas AAD, Henriques JCC. Turbine-generator set laboratory tests in variable unidirectional flow. Open Sea Operating Experience to Reduce Wave Energy Costs, Deliverable 2017;D3(2). Tech. rep., OPERA - URL:http://opera-h2020.eu/wp-content/uploads/2016/03/OPERA_D3-2_Dry_Testing_IST.pdf.
[72] Falcão AFO. Control of an oscillating-water-column wave power plant for maximum energy production. Appl Ocean Res 2002;24(2):73–82. https://doi.org/10.1016/S0141-1187(02)00021-4.
[73] Mosquera FD, Evangelista CA, Puleston PF, Ringwood JV. Optimal wave energy extraction for oscillating water columns using second-order sliding mode control. IET Renew Power Gener 2020;14(9):1512–9. https://doi.org/10.1049/iet-rpg.2019.1392.
[74] Strati FM, Malara G, Arena F. Performance optimization of a U-oscillating-water-column wave energy harvester. Renewable Energy 2016;99:1019–28. https://doi.org/10.1016/j.renene.2016.07.080.
[75] Gaebele DT, Magaña ME, Brekken TKA, Henriques JCC, Carrelhas AAD, Gato LMC. Second order sliding mode control of oscillating water column wave energy converters for power improvement. IEEE Trans Sustain Energy 2021;12 (2):1151–60. https://doi.org/10.1109/TSTE.2020.3035501.
[76] P.A.P. Justino, A.F. de O. Falcão, Rotational Speed Control of an OWC Wave Power Plant, J Offshore Mech Arct Eng 121(2) (1999) 65–70. doi:10.1115/1.2830079.
[77] Ceballos S, Rea J, Lopez I, Pou J, Robles E, O'Sullivan DL. Efficiency optimization in low inertia Wells turbine-oscillating water column devices. IEEE Trans Energy Convers 2013;28(3):553–64. https://doi.org/10.1109/TEC.2013.2265172.
[78] Amundarain M, Alberdi M, Garrido AJ, Garrido I. Modeling and simulation of wave energy generation plants: Output power control. IEEE Trans Industr Electron 2011;58(1):105–17. https://doi.org/10.1109/TIE.2010.2047827.
[79] Alberdi M, Amundarain M, Garrido A, Garrido I, Casquero O, De la Sen M. Complementary control of oscillating water column-based wave energy conversion plants to improve the instantaneous power output. IEEE Trans Energy Convers 2011;26(4):1021–32. https://doi.org/10.1109/TEC.2011.2167332.
[80] Garrido I, Garrido AJ, Alberdi M, Amundarain M, Barambones O. Performance of an ocean energy conversion system with dfig sensorless control. Math Probl Eng 2013. https://doi.org/10.1155/2013/260514.
[81] K. Ezhilsabareesh, R. Suchithra, A. Samad, Performance enhancement of an impulse turbine for OWC using grouped grey wolf optimizer based controller, Ocean Eng doi:10.1016/j.oceaneng.2019.106425.
[82] F. M'zoughi, S. Bouallegue, A.J. Garrido, I. Garrido, M. Ayadi, Stalling-free control strategies for oscillating-water-column-based wave power generation plants, IEEE Trans Energy Convers 33 (1) (2017) 209–222. doi:10.1109/TEC.2017.2737657.
[83] F. M'zoughi, I. Garrido, S. Bouallègue, M. Ayadi, A.J. Garrido, Intelligent airflow controls for a stalling-free operation of an oscillating water column-based wave power generation plant, Electronics 8 (1) (2019) 70. doi:10.3390/electronics8010070.
[84] Amundarain M, Alberdi M, Garrido A, Garrido I. Neural rotational speed control for wave energy converters. Int J Control 2011;84(2):293–309. https://doi.org/10.1080/00207179.2010.551141.
[85] F. M'zoughi, I. Garrido, A.J. Garrido, M. De La Sen, Rotational speed control using ANN-based MPPT for OWC based on surface elevation measurements, Appl Sci 10 (24). doi:10.3390/app10248975.
[86] F. M'zoughi, I. Garrido, A.J. Garrido, M. De La Sen, Self-adaptive global-best harmony search algorithm-based airflow control of a wells-turbine-based oscillating-water column, Appl Sci 10 (13). doi:10.3390/app10134628.
[87] F. M'zoughi, I. Garrido, A.J. Garrido, Symmetry-breaking for airflow control optimization of an oscillating-water-column system, Symmetry 12 (6). doi:10.3390/sym12060895.
[88] F. M'zoughi, I. Garrido, A.J. Garrido, M. De La Sen, ANN-based airflow control for an oscillating water column using surface elevation measurements, Sensors 20 (5). doi:10.3390/s20051352.
[89] Ceballos S, Rea J, Robles E, Lopez I, Pou J, O'Sullivan D. Control strategies for combining local energy storage with wells turbine oscillating water column devices. Renewable Energy 2015;83:1097–109. https://doi.org/10.1016/j.renene.2015.05.030.
[90] Utkin VI. Sliding mode control design principles and applications to electric drives. IEEE Trans Ind Electron 1993;40(1):23–36. https://doi.org/10.1109/41.184818.
[91] M.E. Magaña, R. Danielle, Sliding mode control of an array of three oscillating water column wave energy converters to optimize electrical power, in: Proceedings of the 13th European Wave and Tidal Energy Conference, Cork, Ireland, 2019. URL: https://par.nsf.gov/biblio/10169074.
[92] F. M'zoughi, A.J. Garrido, I. Garrido, S. Bouallègue, M. Ayadi, Sliding mode rotational speed control of an oscillating water column-based wave generation power plants, in: 2018 International Symposium on Power Electronics, Electrical Drives, Automation and Motion (SPEEDAM), IEEE, 2018, pp. 1263–1270. doi:10.1109/SPEEDAM.2018.8445229.
[93] F. M'zoughi, I. Garrido, A.J. Garrido, M. De la Sen, Fuzzy gain scheduled-sliding mode rotational speed control of an oscillating water column, IEEE Access 8 (2020) 45853–45873. doi:10.1109/ACCESS.2020.2978147.
[94] Faedo N, Olaya S, Ringwood JV. Optimal control, MPC and MPC-like algorithms for wave energy systems: An overview. IFAC J Syst Control 2017;1:37–56. https://doi.org/10.1016/j.ifacsc.2017.07.001. URL:https://www.sciencedirect.com/science/article/pii/S2468601817301104.
[95] Rajapakse G, Jayasinghe S, Fleming A, Negnevitsky M. A model predictive control-based power converter system for oscillating water column wave energy converters. Energies 2017;10(10):1631–48. https://doi.org/10.3390/en10101631.
[96] Blanco M, Ramirez D, Zarei ME, Gupta M. Dual multivector model predictive control for the power converters of a floating OWC WEC. Int J Electr Power Energy Syst 2021;133:107263. https://doi.org/10.1016/j.ijepes.2021.107263.
[97] Mishra SK, Purwar S, Kishor N. An optimal and non-linear speed control of oscillating water column wave energy plant with wells turbine and DFIG. Int J Renew Energy Res 2016;6(3):995–1006. URL:https://www.researchgate.net/publication/307862955_An_Optimal_and_Non-Linear_Speed_Control_of_Oscillating_Water_Column_Wave_Energy_Plant_with_Wells_Turbine_and_DFIG.
[98] Mishra SK, Appasani B, Jha AV, Garrido I, Garrido AJ. Centralized airflow control to reduce output power variation in a complex OWC ocean energy network. Complexity 2020. https://doi.org/10.1155/2020/2625301.
[99] C. Napole, O. Barambones, M. Derbeli, J.A. Cortajarena, I. Calvo, P. Alkorta, P.F. Bustamante, Double fed induction generator control design based on a fuzzy logic controller for an oscillating water column system, Energies 14 (12). doi:10.3390/en14123499.
[100] J. Falnes, Optimum control of oscillation of wave-energy converters, Int J Offshore Polar Eng 12 (02). URL: https://onepetro.org/ISOPEIOPEC/proceedings-abstract/ISOPE01/All-ISOPE01/ISOPE-I-01-085/7959.
[101] Ringwood JV. Wave energy control: Status and perspectives 2020. IFAC-PapersOnLine 2020;53(2):12271–82. https://doi.org/10.1016/j.ifacol.2020.12.1162.
[102] D. García-Violini, N. Faedo, F. Jaramillo-Lopez, J.V. Ringwood, Simple controllers for wave energy devices compared, J Mar Sci Eng 8 (10). doi:10.3390/jmse8100793. URL: https://www.mdpi.com/2077-1312/8/10/793.
[103] Sarmento AJNA, Gato LMC, Falcão AFO. Turbine-controlled wave energy absorption by oscillating water column devices. Ocean Eng 1990;17(5):481–97. https://doi.org/10.1016/0029-8018(90)90040-D.
[104] Perdigao J, Sarmento A. Overall-efficiency optimisation in OWC devices. Appl Ocean Res 2003;25(3):157–66. https://doi.org/10.1016/j.apor.2003.09.002.

[105] Korde UA. Development of a reactive control apparatus for a fixed two-dimensional oscillating water column wave energy device. Ocean Eng 1991;18 (5):465–83. https://doi.org/10.1016/0029-8018(91)90026-M.
[106] Henriques JCC, Gato LMC, Falcão AFO, Robles E, Faÿ F-X. Latching control of a floating oscillating-water-column wave energy converter. Renewable Energy 2016;90:229–41. https://doi.org/10.1016/j.renene.2015.12.065.
[107] Budal K, Falnes J. Wave power conversion by point absorbers: A norwegian project. Int J Ambient Energy 1982;3(2):59–67. https://doi.org/10.1080/01430750.1982.9675829.
[108] R.E. Hoskin, B.M. Count, N.K. Nichols, D.A.C. Nicol, Phase control for the oscillating water column, in: D.V. Evans, A.F.O. Falcão (Eds.), IUTAM Symp. Hydrodynamics of Ocean-Wave Energy Utilisation, Springer-Verlag, 1986, pp. 257–268. doi:10.1007/978-3-642-82666-5_22.
[109] R. Jefferys, T. Whittaker, Latching control of an oscillating water column device with air compressibility, in: D.V. Evans, A.F.O. Falcão (Eds.), IUTAM Symp. Hydrodynamics of Ocean-Wave Energy Utilisation, Springer-Verlag, 1986, pp. 281–291. doi:10.1007/978-3-642-82666-5_24.
[110] S. Salter, J. Taylor, The design of a high-speed stop valve for oscillating water columns, in: Proceedings of the 2nd European Wave Power Conference, vol. 3, Lisbon, Portugal, 1996, pp. 195–202.
[111] Henriques JCC, Lemos JM, Eça L, Gato LMC, Falcão AFO. A high-order Discontinuous Galerkin Method with mesh refinement for optimal control. Automatica 2017;85:70–82. https://doi.org/10.1016/j.automatica.2017.07.029.
[112] Paparella F, Monk K, Winands V, Lopes MFP, Conley D, Ringwood JVV. Up-wave and autoregressive methods for short-term wave forecasting for an oscillating water column. IEEE Trans Sustain Energy 2015;6(1):171–8. https://doi.org/10.1109/TSTE.2014.2360751.
[113] J. Marques Silva, S.M. Vieira, D. Valério, J.C.C. Henriques, P.D. Sclavounos, Air pressure forecasting for the mutriku oscillating-water-column wave power plant: Review and case study, IET Renew Power Gener 15 (14) (2021) 3485–3503. doi:10.1049/rpg2.12289.
[114] J.C.C. Henriques, A.F.O. Falcão, R.P.F. Gomes, L.M.C. Gato, Latching control of an oscillating water column spar-buoy wave energy converter in regular waves, J Offshore Mech Arctic Eng 135 (2). doi:10.1115/1.4007595.
[115] Henriques JCC, Chong JC, Falcão AFO, Gomes RPF. Latching control of a floating oscillating water column wave energy converter in irregular waves. In: Proceedings of the International Conference on Ocean, Offshore and Arctic Engineering. San Francisco, California, USA; 2014. https://doi.org/10.1115/OMAE2014-23260.
[116] Henriques JCC, Gato LMC, Lemos JM, Gomes RPF, Falcão AFO. Peak-power control of a grid-integrated oscillating water column wave energy converter. Energy 2016;109:378–90. https://doi.org/10.1016/j.energy.2016.04.098.
[117] Babarit A, Guglielmi M, Clément AH. Declutching control of a wave energy converter. Ocean Eng 2009;36(12–13):1015–24. https://doi.org/10.1016/j.oceaneng.2009.05.006.
[118] Salter SH, Taylor JRM, Caldwell NJ. Power conversion mechanisms for wave energy. Proc Inst Mech Eng, Part M: J Eng Maritime Environ 2002;216(1):1–27. https://doi.org/10.1243/147509002320382103.
[119] Henriques JCC, Gomes RPF, Gato LMC, Falcão AFO, Robles E, Ceballos S. Testing and control of a power take-off system for an oscillating-water-column wave energy converter. Renewable Energy 2016;85:714–24. https://doi.org/10.1016/j.renene.2015.07.015.
[120] C. Roh, K.-H. Kim, Deep learning prediction for rotational speed of turbine in oscillating water column-type wave energy converter, Energies 15 (2). doi:10.3390/en15020572.
[121] Garrido AJ, Garrido I, Amundarain M, Alberdi M, De la Sen M. Sliding-mode control of wave power generation plants. IEEE Trans Ind Appl 2012;48(6):2372–81. https://doi.org/10.1109/TIA.2012.2227096.
[122] Barambones O, Gonzalez de Durana JM, Calvo I. Adaptive sliding mode control for a double fed induction generator used in an oscillating water column system. Energies 2018;11(11):2939. https://doi.org/10.3390/en11112939.
[123] Mishra SK, Purwar S, Kishor N. Event-triggered nonlinear control of OWC ocean wave energy plant. IEEE Trans Sustain Energy 2018;9(4):1750–60. https://doi.org/10.1109/TSTE.2018.2811642.
[124] R. Suchithra, K. Ezhilsabareesh, A. Samad, Optimization based higher order sliding mode controller for efficiency improvement of a wave energy converter, Energy 187. doi:10.1016/j.energy.2019.116111.
[125] D.T. Gaebele, M.E. Magaña, T.K.A. Brekken, J.C.C. Henriques, Constrained sliding mode control for oscillating water column wave energy converters., IFAC-PapersOnLine 53 (2) (2020) 12327–12333. doi:10.1016/j.ifacol.2020.12.1202.
[126] Song S-K, Park J-B. Modeling and control strategy of an oscillating water column-wave energy converter with an impulse turbine module. In: Proceedings of the 15th International Conference on Control. Busan, Korea: Automation and Systems; 2015. p. 1983–8. https://doi.org/10.1109/ICCAS.2015.7364693.
[127] Song SK, Park JB. Control strategy of an impulse turbine for an oscillating water column-wave energy converter in time-domain using lyapunov stability method. Appl Sci 2016;6(10):281. https://doi.org/10.3390/app6100281.
[128] Korde UA. A power take-off mechanism for maximizing the performance of an oscillating water column wave energy device. Appl Ocean Res 1991;13(2):75–81. https://doi.org/10.1016/S0141-1187(05)80064-1.
[129] Hardy P, Cazzolato BS, Ding B, Prime Z. A maximum capture width tracking controller for ocean wave energy converters in irregular waves. Ocean Eng 2016;121:516–29. https://doi.org/10.1016/j.oceaneng.2016.05.045.
[130] Faÿ F-X, Marcos M, Robles E. Novel predictive latching control for an oscillating water column buoy. In: Proceedings of the 12th European Wave and Tidal Energy Conference. Cork, Ireland; 2017. URL:https://www.researchgate.net/publication/319465535_Novel_Predictive_Latching_Control_for_an_Oscillating_Water_Column_Buoy.
[131] Said HA, Ringwood JV. Grid integration aspects of wave energy–overview and perspectives. IET Renew Power Gener 2021;15(14):3045–64. https://doi.org/10.1049/rpg2.12179.
[132] Alberdi M, Amundarain M, Garrido AJ, Garrido I, Maseda FJ. Fault-ride-through capability of oscillating-water-column-based wave-power-generation plants equipped with doubly fed induction generator and airflow control. IEEE Trans Industr Electron 2010;58(5):1501–17. https://doi.org/10.1109/TIE.2010.2090831.
[133] Alberdi M, Amundarain M, Garrido A, Garrido I. Neural control for voltage dips ride-through of oscillating water column-based wave energy converter equipped with doubly-fed induction generator. Renewable Energy 2012;48:16–26. https://doi.org/10.1016/j.renene.2012.04.014.
[134] Ramirez D, Blanco M, Zarei ME, Gupta M. Robust control of a floating OWC WEC under open-switch fault condition in one or in both VSCs. IET Renew Power Gener 2020;14(13):2538–49. https://doi.org/10.1049/iet-rpg.2020.0203.
[135] Zarei ME, Ramírez D, Nicolas CV, Arribas JR. Three-phase four-switch converter for SPMS generators based on model predictive current control for wave energy applications. IEEE Trans Power Electron 2019;35(1):289–302. https://doi.org/10.1109/TPEL.2019.2911209.
[136] Zarei ME, Ramirez D, Veganzones C, Rodriguez J. Predictive direct control of SPMS generators applied to the machine side converter of an OWC power plant. IEEE Trans Power Electron 2020;35(7):6719–31. https://doi.org/10.1109/TPEL.2019.2956738.
[137] Murray DB, Hayes JG, O'Sullivan DL, Egan MG. Supercapacitor testing for power smoothing in a variable speed offshore wave energy converter. IEEE J Oceanic Eng 2012;37(2):301–8. https://doi.org/10.1109/JOE.2012.2188157.
[138] G. Rajapakse, S. Jayasinghe, A. Fleming, M. Negnevitsky, Grid integration and power smoothing of an oscillating water column wave energy converter, Energies 11 (7). doi:10.3390/en11071871.
[139] Senjyu T, Sakamoto R, Urasaki N, Funabashi T, Fujita H, Sekine H. Output power leveling of wind turbine generator for all operating regions by pitch angle control. IEEE Trans Energy Convers 2006;21(2):467–75. https://doi.org/10.1109/TEC.2006.874253.
[140] Baillieul J, Samad T. Encyclopedia of systems and control. Springer; 2021.
[141] Fusco F, Ringwood JV. Hierarchical robust control of oscillating wave energy converters with uncertain dynamics. IEEE Trans Sustain Energy 2014;5(3):958–66. https://doi.org/10.1109/TSTE.2014.2313479.
[142] Garcia-Violini D, Ringwood JV. Energy maximising robust control for spectral and pseudospectral methods with application to wave energy systems. Int J Control 2021;94(4):1102–13. https://doi.org/10.1080/00207179.2019.1632491.
[143] Faedo N, García-Violini D, Scarciotti G, Astolfi A, Ringwood JV. Robust moment-based energy-maximising optimal control of wave energy converters. In: 2019 IEEE 58th Conference on Decision and Control (CDC), IEEE; 2019. p. 4286–91. https://doi.org/10.1109/CDC40024.2019.9029578.
[144] Rezanejad K, Gadelho JFM, López I, Carballo R, Guedes Soares C. Improving the Hydrodynamic Performance of OWC Wave Energy Converter by Attaching a Step. In: Proceedings of the 38th International Conference on Offshore Mechanics and Arctic Engineering. Glasgow, Scotland, UK; 2019. https://doi.org/10.1115/OMAE2019-96408.
[145] Çelik A. An experimental investigation into the effects of front wall geometry on OWC performance for various levels of applied power take off dampings. Ocean Eng 2022;248:110761. https://doi.org/10.1016/j.oceaneng.2022.110761.
[146] Garcia-Rosa PB, Ringwood JV. On the sensitivity of optimal wave energy device geometry to the energy maximizing control system. IEEE Trans Sustain Energy 2015;7(1):419–26. https://doi.org/10.1109/TSTE.2015.2423551.
[147] Garrido AJ, Garrido I, Alberdi M, Amundarain M, Barambones O, Romero JA. Robust control of oscillating water column (OWC) devices: Power generation improvement. 2013 OCEANS-San Diego, IEEE 2013;2013:1–4. https://doi.org/10.23919/OCEANS.2013.6740982.